# Thermal fluctuations independently modulate physiological plasticity and the dynamics of the gut microbiome in a tropical rocky shore oyster

Bovern Suchart Arromrak, Adrian Tsz Chun Wong, Tin Yan Hui, Kin Sum Leung, Gray A Williams, Monthon Ganmanee, Thierry Durand, Jetty Chung-Yung Lee, Juan Diego Gaitan-Espitia

# Thermal fluctuations independently modulate physiological plasticity and the dynamics of the gut microbiome in a tropical rocky shore oyster

Bovern Suchart Arromrak[1]; Adrian Tsz Chun Wong[1]; Tin Yan Hui[1]; Kin Sum Leung[1]; Gray A. Williams[1]; Monthon Ganmanee[2]; Thierry Durand[3]; Jetty Chung Yung Lee[4]; & Juan D. Gaitan-Espitia[1*]

[1] The Swire Institute of Marine Science and School of Biological Sciences, The University of Hong Kong, Hong Kong, SAR, China.
[2] Department of Animal Production Technology and Fisheries, Faculty of Agricultural Technology, King Mongkut's Institute of Technology Ladkrabang, Bangkok 10520, Thailand
[3] Institut des Biomolécules Max Mousseron (IBMM), Pôle Chimie Balard Recherche, UMR 5247, Université de Montpellier, CNRS, ENSCM, F-34293 Montpellier Cedex 05, France
[4] School of Biological Sciences, The University of Hong Kong, Hong Kong, SAR, China

*** Correspondence**: juadiegaitan@gmail.com

# Abstract

Extreme high thermal conditions on rocky shores are challenging to the survival of intertidal ectotherms. Yet, many species are highly successful in these environments in part due to their ability to regulate intrinsic mechanisms associated with physiological stress and their metabolic demand. More recently, there has been a growing awareness that other extrinsic mechanisms, such as animal-associated microbial communities, can also influence the tolerance and survival of ectotherms under stressful conditions. However, the extent to which the intrinsic and extrinsic mechanisms are functionally linked as part of the overall adaptive response of intertidal animals to temperature change and stress is poorly understood. Here, we examined the dynamics and potential interactions of intrinsic and extrinsic mechanisms in the tropical high-supratidal oyster, *Isognomon nucleus*. We found that oysters modulate their internal biochemistry (oxidized PUFA products including 5-$F_{2t}$-IsoP, 10-$F_{4t}$-NeuroP, 13-$F_{4t}$-NeuroP, and 16-$F_{1t}$-PhytoP) as part of their adaptive regulation to cope with physiological stress during periods of extreme high temperatures when emersed. While we detected extrinsic microbiome changes in alpha diversity (ASV richness and Shannon diversity index), the overall taxonomic and functional structure of the microbiome based on beta-diversity analysis (PERMANOVA) showed temporal stability and no association with the host biochemical profiles. Our finding here suggests that the microbiome taxonomic and functional structure is potentially maintained by a stable host control (not associated to the host biochemistry) and/or that the microbiome (independent of the host) is resilient to the local thermal fluctuations and extreme high temperature experienced. This microbiome stability is likely to contribute to the oyster, *I. nucleus* thermal tolerance, in addition to the intrinsic biochemical responses, to survive in the thermally challenging intertidal environment.



Keywords: Phenotypic plasticity, ectotherms, microbiome, thermal stress

# Introduction

The tropical rocky shore is one of the most extreme environments on Earth. This system is characterised by a marked heterogeneous thermal landscape influenced by tidal dynamics (Raffaelli and Hawkins, 1999; Helmuth and Hofmann, 2001). Across this vertical gradient defined by the tides, environmental temperatures shape the physiology, behaviour, and spatial distribution of tropical intertidal ectotherms (Garrity, 1984; Williams and Morritt, 1995; Chow, 2004; Samakraman *et al.*, 2010; Giomi *et al.*, 2016; Ng *et al.*, 2017). For ectotherms occupying the high-supratidal zone, thermal and oxidative stress (i.e., excessive production of reactive oxygen species - ROS) during desiccation periods of extended emersion, are the two of the major physiological challenges faced (Sokolova and Pörtner, 2001; Freire *et al.*, 2011; Birben *et al.*, 2012).

To survive under these challenging conditions, high-supratidal ectotherms modulate intrinsic/innate mechanisms associated with their internal physiology (e.g., metabolic rate) and biochemical activities. This modulation can be observed through, for instance, the removal of ROS via polyunsaturated fatty acids (PUFA; Sokolova and Pörtner, 2001; Yin *et al.*, 2017; Monroig *et al.*, 2022), and/or the control of the gene expression associated with heat shock response (HSR) and oxidative stress response (OSR; Wang *et al.*, 2022). PUFAs such as Arachidonic acid (ARA) and Docosahexaenoic acid (DHA) are known to be effective molecules and agent for ROS removal, because they contain unsaturated double bonds making them susceptible to ROS reaction (particularly to peroxide, HO•) (Sargent, 1976; Leung *et al.*, 2015; Yin *et al.*, 2017; Fadhlaoui and Lavoie, 2021). The non-enzymatic peroxidation of these PUFAs, generates by-products that can be used as biomarkers of the ROS level (Miller *et al.*, 2014; Yonny *et al.*, 2016; Galano *et al.*, 2017). In addition to the biochemical modulation mechanism, some intertidal organisms (e.g., the oysters, *Isognomon nucleus*) are able to enter into a hypometabolic state (i.e., metabolic depression, for instance, marked by a drop in heart

80 rate; Marshall and McQuaid, 2011; Hui *et al.*, 2020) to avoid excessive energy consumption
81 when exposed to high temperatures during low tides. Together, these functional characteristics
82 are regarded as important adaptive traits for intertidal ectotherms to cope and ameliorate the
83 extreme stress experienced on tropical rocky shores.

84 Survival under stressful environmental conditions is also hypothesized to be influenced
85 by extrinsic/acquired mechanisms such as host-associated microbial communities (i.e.,
86 microbiome; Bang *et al.*, 2018; Ahmed *et al.*, 2019). The structure and functions of these
87 microbiomes have been suggested to play important roles in shaping tolerances and
88 biochemical regulation of animals to elevated temperatures (Herrera *et al.*, 2020; Sepulveda
89 and Moeller, 2020; Jaramillo and Castañeda, 2021). Under such conditions, functional
90 microbiomes that are resilient/responsive to environmental changes are fundamental to the
91 host's health and survival (Soen, 2014; Kremer *et al.*, 2018). For instance, Epstein et al. (2019)
92 demonstrated that the resilience of the coral, *Pocillopora acuta,* to a stressful thermal event
93 may be attributed to the stability of the microbiome composition and structure. In contrast, a
94 dysbiotic host state is commonly associated with a destabilized microbiome (Fan *et al.*, 2013;
95 McDevitt-Irwin *et al.*, 2019). This is typically reflected by a marked variation among host-
96 associated microbiomes, a signal indicating the host losing control of the microbial community
97 (e.g., increase in opportunistic pathogens) and/or differential sensitivities of microbiomes to
98 extreme disturbances (e.g., elevated temperature; Carey and Duddleston, 2014; Petersen and
99 Round, 2014; Lokmer and Wegner, 2015). This pattern is in-line with the "Anna Karenina
100 Principle", which states, "all happy families are all alike; each unhappy family is unhappy in
101 its own way" (Zaneveld *et al.*, 2017; Díaz-Almeyda *et al.*, 2022). In other words, stressed
102 organisms may host more stochastic microbiomes than healthy organisms. Although
103 microbiome stability seems important for host homeostasis, some studies have suggested that
104 flexibility in the microbiome can also provide adaptive capacities to the host, allowing it to

cope with rapidly changing environments (Maher *et al.*, 2020; Voolstra and Ziegler, 2020). Ziegler et al. (2017), for example, showed that the coral *Acropora hyacinthus* exhibits changes in its microbiome composition and structure that are aligned with the local thermal environmental conditions. Similarly, several studies have also shown seasonal variation in the host-associated microbiome of many marine organisms such as bivalves and echinoderms, as a potential plastic/flexible response to environmental change (Pierce and Evan, 2019; Feng *et al.*, 2021). Microbiome stability or flexibility may, therefore, be a sign of host adaptive responses to environmental changes. However, the influence of these contrasting patterns is context-dependent and thus, their contribution to the tolerances and survival of animal hosts may differ in thermally challenging environments such as tropical rocky shores.

Previous studies have shown that the capacity for plastic adaptive responses of animal hosts to environmental stress may be modulated by the interactions between intrinsic (physiology and biochemical changes of the host) and extrinsic (host's microbiome structure and function) mechanisms (Muñoz *et al.*, 2019; Marangon *et al.*, 2021; Fontaine and Kohl, 2023). It is unclear, however, to what extent these mechanisms are functionally linked as part of the whole organism's adaptive response (i.e., holobiont: host and microbiome) to survive in an extreme environment such as the tropical intertidal rocky shore. In this study, we investigated the intrinsic and extrinsic mechanisms underpinning tolerances and survival of a tropical intertidal ectotherm (oyster, *Isognomon nucleus*) by assessing the influence of natural variation in environmental temperature on i) host physiology (i.e., biochemical dynamics) ii) the diversity, structure, and function of the host gut-associated microbiome and iii) the interplay between these mechanisms. The integration of intrinsic and extrinsic mechanisms offers a holobiont perspective for understanding the stress tolerance regulation of ectotherms in extreme high temperature and fluctuating environments (Alberdi *et al.*, 2016; Apprill, 2017; Bang *et al.*, 2018).

# Materials and methods

## *Site and species descriptions*

Host-microbiome interactions were investigated in the oyster, *Isognomon nucleus* (Bivalvia: Isognomonidae), a dominant ectotherm of the high-supratidal zone in Southeast Asia. Animals were collected from Ko Sichang, Thailand (latitude: 13°08'52''N; longitude: 100°48'11''E). In this area, *I. nucleus* is abundant and forms a distinctive band at the high-supratidal zone (~2.5 - 3 m above the mean sea level; Samakraman *et al.*, 2010), where rock temperatures vary daily (emersion period) from ~30°C at dawn to ~50°C at noon (hot season: March to June; Hui *et al.*, 2020). The oyster exhibits strong variations in physiological and metabolic adjustments with elevated body temperatures, providing an ideal system to investigate the functional role of the microbiome to facilitate the host's survival in this thermally extreme and variable environment (Giomi *et al.*, 2016; Hui *et al.*, 2020).

## *Sample collection and processing*

A total of 80 individuals of *I. nucleus* were randomly selected at four different timepoints within an emersion period (Fig. 1A; 20 animals at each time) with contrasting thermal conditions (09:15 hr, 12:30 hr, 16:12 hr, and 17:40 hr; hereafter, morning, noon, early-afternoon, and late-afternoon, respectively; Table S1). This cycle represents major changes in the environmental temperature as a result of the tidal dynamics and air/sun exposure (Hui *et al.*, 2020). Body temperatures were measured from 10 randomly selected individuals at each timepoint using a digital thermometer (± 0.1 °C, TM-947SD, Lutron, Taiwan) where a fine-tipped type-K thermocouple was inserted into the bodies through the valve opening. At each time point, the whole tissue of five collected oysters was quickly removed at the site with a sterile dissecting kit and snap-frozen in liquid nitrogen on shore for oxidative stress quantification (as a proxy for host physiological and biochemical dynamics). The guts of

another five individuals were also dissected at each timepoint on-site, snap frozen in liquid nitrogen for gut microbiome assessment. All collected samples (20 for oxidative stress and 20 for microbiome analysis across four time points) were stored in a portable liquid nitrogen tank and transported to The University of Hong Kong within three days, where they were held in a -80°C freezer until processing and analyses. Because of the weather instability and strong waves during the fieldwork, temporal sampling was limited to one day to comply with logistic and safety regulations.

### *Rock surface temperature and tidal dynamics*

To quantify environmental conditions experienced by *Isognomon nucleus* throughout the tidal cycle, rock surface temperatures and tidal levels were recorded. To measure and track surface rock temperature, i-Button loggers (DS1922L, Maxim, US) were firstly embedded in waterproofing resin (Scotchcast, 3M, US), placed in plastic Falcon tube caps and affixed, using marine epoxy (A-788, Z-Spar, US; Ng *et al.*, 2021), onto the shore at the height where *I. nucleus* were collected. Rock surface temperatures were logged by these i-Buttons every 5 minutes at a resolution of 0.5 °C (n = 5). Additionally, a time-lapse camera (TLC200Pro, Brinno, Taiwan) was set adjacent to the study site to monitor the immersion state of the *I. nucleus* band during the day (~ 05:00 hr to 18:00 hr) to assess the tidal states. Images were captured every 10 minutes and the tidal level was scored according to whether the band was underwater (immersed), exposed to air (emersed), or being splashed by waves during transitions from immersion/emersion (awash). During the emersion period, animals showed no intermittent gaping (Hui, T.Y., unpublished data). Predicted tide height from the lowest low water height on the sampling date was also obtained from the Hydrographic Department, Royal Thai Navy Website (https://www.hydro.navy.mi.th/index1.php#nogo2): Lowest tidal height - 0.55m (12:56 hr) and highest tidal height - 3.36m (20:53hr).

*Determination of polyunsaturated fatty acids-oxidized metabolites*

The levels of oxidative stress (i.e., associated with ROS production) of the oysters were determined based on the concentration of non-enzymatic oxidized polyunsaturated fatty acids (PUFA) products (hereafter, oxidized PUFA products; Durand *et al.*, 2009; Basu, 2010; Leung *et al.*, 2015). A modified Folch extraction method was used to extract the oxidized PUFA products from the oysters sampled (n=5) at each timepoint (t=4) (Folch *et al.*, 1957; Dupuy *et al.*, 2016). In brief, 0.05g of oyster flesh was suspended in a 5 ml ice-cold Folch solution (chloroform: methanol, 2:1, v/v) with 0.01% Butylated HydroxyToluene (BHT; used as anti-oxidant to prevent lipid peroxidation during sample processing) (w/v) and homogenized at 24,000 rpm in 20 secs bursts on ice using a polytron benchtop homogenizer (T25, Ultra-Turrax, IKA, Germany). Homogenization was performed twice, and the two parts of the Folch solution extracts were pooled. The pooled solutions were added with 2 ml of 0.9% NaCl to introduce phase separation. The mixture was then shaken on ice for 30 min and centrifuged at 2000 × g for 10 min at room temperature. The lower chloroform phase was transferred into a 30 ml glass vial. The extracted samples were then added with potassium hydroxide (1M in methanol) and 1X PBS (pH7.4). Samples were then shaken overnight in the dark at room temperature for alkaline hydrolysis of the extracted samples. This step is required to obtain free forms of fatty acids by deacylation of phospholipid (most lipids exist in this form) from the extracted samples. The reaction was terminated by adding 1M of hydrochloric acid, methanol, 20 mM of formic acid, and 40 mM of formic acid. Deuterated internal standards (5ng prepared in methanol) were also added after the hydrolysis. Purification of the oxidized PUFA metabolites was performed with the mixed anion solid phase extraction (MAX SPE, Waters, Milford, MA USA). Before the start of the solid phase extraction, the SPE column was preconditioned with methanol and 20 mM formic acid. One sample was then loaded into a column and cleaned with 2% ammonium hydroxide and 20 mM formic acid. The final eluent was collected with

hexane/ethanol/acetic acid (70/29.4/0.6, v/v/v). All the samples were then placed on a heating block and heated at 37°C under a stream of nitrogen gas until they were completely dried. The dried samples were then re-suspended in 100 µL methanol and cleaned through a 0.45 µm PTFE filter to remove insoluble impurities, and then immediately analysed by liquid chromatography-tandem mass spectrometry (LC-MS/MS).

In our study, we used the Sciex X500R QTOF LC-MS/MS system (Sciex Applied Biosystems, MA, USA) which consisted of an Exion LC liquid chromatography with a C18 column (150×2.1 mm, 2.6 µm particle size, Phenomenex, Torrance, CA, USA) which was maintained at 40°C for LC-MS/MS analysis. A mobile phase consisting of 0.1% aqueous acetic acid (solvent A) and 0.1% acetic acid/methanol (solvent B) was used. The flow rate was set to 300 µl/min and the injection volume to 10 µl. For each sample analysis, the gradient condition was maintained at 20% of solvent B for 2 min and between 20% and 98% for 8 min and then held for 5 min. Then, the percentage of solvent B was reduced to 20% in 1 min and held for an additional 5 min to equilibrate to the initial conditions. The X500R QTOF system was operated in negative electrospray ionization (ESI) mode. The spray voltage was set to -4500V and nitrogen was used as the curtain gas. The ionization chamber temperature was set at 350°C, and the pressure of the ion source gases 1 and 2 were 35 and 45 psi, respectively. The declustering potential (DP) was set to -80V and the collision energy (CE) was -10V for the QTOF MS. The scan mode was set to multiple reaction monitoring (MRM). All data collected by the X500R QTOF system was analyzed by the Sciex operating system (version 1.2.0.4122). The quantification of each analyte was determined by correlating the peak area to its corresponding deuterated internal standard peak. For analytes without corresponding deuterated internal standards, the following deuterated internal standards, 5(*S*)-HETE-$d_8$, 15-$F_{2t}$-IsoP-$d_4$, and 4-$F_{4t}$-NeuroP-$d_4$ were used for quantification. We identified fifteen oxidized PUFA products that are

known to be the products of non-enzymatic lipid peroxidation (Table S2), based on previous work by Dupuy et al.(2016), Galano et al.(2017) and Lee et al.(2018).

### *DNA extraction and 16S rRNA gene sequencing*

Total genomic DNA was extracted from the oysters' guts (~0.03g) using the commercial DNA extraction kit, Dneasy Power Soil Kit (Qiagen GmbH, Hilden, Germany), following the manufacturers protocol with some modifications (i.e., the solution mixture was incubated at 55℃ in a water bath for 30 minutes after the bead-beating step). The extracted DNA (100µl) was then collected in a microcentrifuge tube and preserved in a -80℃ freezer. All the DNA samples were then sent to Ramaciotti Centre for Genomics at the University of New South Wales, Sydney Australia for 16S rRNA amplicon paired-end sequencing (2X 300bp) on an Illumina Miseq Platform. Before the amplicon sequencing, the V3-V4 variable region of the 16S rRNA gene from each DNA sample was amplified using the following primers: (1) 341F (Forward Primer);5'- CCTACGGGNGGCWGCAG-3' (2) 805R (Reverse Primer); 5'-GACTACHVGGGTATCTAATCC-3'(Herlemann *et al.*, 2011; Klindworth *et al.*, 2013). Raw reads received were the demultiplexed paired-end sequences in a FASTQ format and they were deposited in NCBI Sequence Read Archive (SRA) under Bioproject number PRJNA931123. The data will be made available once published.

### *16S rRNA gene sequence processing*

Raw demultiplexed paired-end sequences were processed following the Quantitative Insights into Microbial Ecology (QIIME2 ver. 2021.4) pipeline (Bolyen *et al.*, 2019). Briefly, the raw data was first visualized with the demux plug-in function for quality-checking and identifying poor-quality base regions to filter. The sequences were then trimmed, filtered, denoised, chimeras-removed, and merged using the DADA2 plug-in function in QIIME2 (Callahan *et al.*, 2016). The sequences were identified at a single nucleotide threshold

(Amplicon Sequence Variants; ASV; Callahan *et al.*, 2017). Additional steps of quality control were performed to reduce non-target sequences by aligning (vsearch alignment method) the ASV sequences to the 99% representative sequences from the greengenes database and only ASV with a similarity threshold of 0.65% and coverage threshold of 0.5% were retained following https://github.com/biocore/deblur/issues/139#issuecomment-282143373. Singletons and sequences with less than 349bp were also removed with filter-features and filter-sets function in QIIME2, respectively. The quality-filtered sequences were then taxonomically assigned with a naïve-Bayes classifier trained on the V3-V4 region of the 16S gene in the Silva v138 database (Quast *et al.*, 2013), using the classify-sklearn function in the feature-classifier plugin (Bolyen *et al.*, 2019). The output from this generated a taxonomy table with taxonomic naming for each ASV found within our samples. ASV sequences that were identified as mitochondria, chloroplast, archaea, and eukaryotes were filtered out. The quality-filtered ASV sequences were then ready to be used for downstream analysis.

### *Profiling microbiome functions*

The functional microbiome was predicted using the software Phylogenetic Investigation Communities by Reconstruction of Unobserved States version 2 (PICRUSt2; Douglas *et al.*, 2020). The predicted functions associated with the microbiome (using the quality-filtered sequences) were inferred based on the MetaCyc pathway abundance, using the PICRUSt plug-in within QIIME2.

### *Data analysis*

Unless otherwise specified, the R statistical programming language (ver. 4.2.0, R Core Team) and R Studio was used to generate graphics and statistical analyses. The oysters' body temperature data violated the statistical assumption of homogeneity of variances (Levene's test, p-value $< 0.05$). Hence, the statistical analysis for this trait across different timepoints was

assessed using a generalized linear model (GLM) with a gamma distribution. The likelihood-ratio chi-square test was used to determine the statistical significance and is indicated if the p-value was < 0.05 (R package "Car"; Fox and Weisberg, 2019). Post-hoc testing for pairwise comparison was made using the estimated marginal means with Tukey's tests from the R package emmeans (Lenth, 2023)

Individual oxidized PUFA products were first evaluated for normality (Shapiro-Wilk's Test) and homogeneity of variance (Levene's test) assumptions. Metabolites that fulfilled both assumptions were tested with one way Analysis of variance (ANOVA) to investigate the variation in metabolites' concentrations across timepoints, followed by *post-hoc* Tukey's Honest significant difference (Tukey's HSD). For metabolites that violated either one of the assumptions, they were evaluated with GLM (gamma distribution) following a similar procedure as with the body temperature datasets.

Assessment of oxidized PUFA products' beta diversity (with all the 15 metabolites or only the 4 significant metabolites) was performed by first generating a Euclidean distance matrix between samples, using normalized metabolites datasets (i.e., autoscaling; van den Berg *et al.*, 2006). Euclidean distance metric was selected as it allows for accurate and reliable analysis for continuous datasets and testing the differences between groups of samples based on the metabolite data (Qi and Voit, 2017; Mallick *et al.*, 2019; Nguyen *et al.*, 2021). A principle Coordinate Analysis (PCoA) plot was then created to visualize the oxidized PUFA products clustering across different timepoints, using the ggplot2 R package (Wickham, 2008). Permutational multivariate analysis of variance (PERMANOVA) was performed with 999 permutations to test for the differences in oxidized PUFA products profile across timepoints (Oksanen *et al.*, 2022). We also performed a permutational multivariate dispersion test (PERMDISP) to assess differences in the dispersion of metabolite profiles between timepoints

with 999 permutations followed by pairwise comparisons. All multivariate metabolites analyses were performed using the package vegan in R (Oksanen *et al.*, 2022).

Oysters' gut microbiome analysis was conducted by first combining the ASV count data, taxonomy table, and metadata into a simplified data matrix for ease of downstream processing, using the phyloseq() function from the phyloseq R package (McMurdie and Holmes, 2013). Rarefaction curves (total ASVs captured against sampling depth) were generated for each sample with the ggrare() function from the ranacapa R package (Kandlikar *et al.*, 2018). All samples approached the asymptote level, indicating that the total ASV richness for each sample has been captured (Fig. S1). Each of the samples was then rarefied to a sampling depth of 21,282 reads (a cut-off that balances the maximum number of sequences retained per sample and minimizing the number of samples removed) for downstream analysis (Weiss *et al.*, 2017; i.e., alpha and beta diversity; McKnight *et al.*, 2019). Using the rarefied data, the microbiome alpha diversity (i.e., the structure of a microbial community with respect to its richness and evenness; Willis, 2019) was determined based on two indices – ASV richness and Shannon-Wiener (H') diversity. ASV richness was calculated with the Base-R function, while Shannon-Wiener (H') diversity index was generated using the diversity() function from the Vegan package (Oksanen *et al.*, 2022). Differences in the microbiome alpha diversity across the timepoints were assessed with ANOVA and followed by a *post-hoc* Tukey HSD test. The ANOVA statistical assumptions of normality (Shapiro-Wilk test) and homogeneity of variance (Levene's test) for all datasets were tested and fulfilled ($p$-value $> 0.05$). Linear regression analysis was also conducted to determine the relationship between the oysters' microbiome alpha diversity (i.e., ASV richness and Shannon-Wiener (H') index) and body temperature (i.e., average of the 10 random independent body temperature replicates collected at each timepoint). The statistical assumptions for the linear regression model were fulfilled based on the normality test (Shapiro-Wilk test) and residuals plot (variance homogeneity).

While alpha diversity focuses on community variation within a community (sample), beta diversity quantifies (dis-)similarites between communities/samples in terms of species presence/absence and abundance (Kers and Saccenti, 2022). Metrics of beta diversity are typically used to measure species turnover or replacement across different locations, environmental conditions or timepoints (Kers and Saccenti, 2022). Here, we assessed beta diversity of the oysters' gut microbiome to evaluate temporal differences in taxonomic and functional structure across all samples simultaneously. Bray-Curtis dissimilarity distance matrix was first generated between all samples. Then, a PCoA plot was created to visualize microbiome taxonomic and functional clusters across different timepoints, using the ggplot2 R package (Wickham, 2008). The chosen dissimilarity distance metric (Bray-Curtis) followed findings by Mcknight et al. (2019) and Weiss et al. (2017), in which authors showed optimal and high confidence for community level comparison with rarefied microbiome datasets. PERMANOVA was performed with 999 permutations to test for the differences in the microbiome composition and structure between timepoints (Oksanen *et al.*, 2022). PERMDISP with 999 permutations was performed to test for differences in the taxonomic and functional microbiome profile dispersion followed by pairwise comparison. All multivariate analyses were conducted using the package vegan in R.

Differential abundance analysis of each microbial taxa was performed with family taxonomic level data (using unrarefied quality-filtered ASV sequences) and analysed with Analysis of Composition Microbiome with Bias Correction (ANCOM-BC) from the ANCOMBC R package (Lin and Peddada, 2020; Nearing *et al.*, 2022). Linear discriminant analysis (LDA) effect size (LEfSe) was performed to screen for differentially abundant predicted microbial function (MetaCyc pathways) across the four timepoints , based on an LDA threshold of 2.0 and a statistical significance cut-off of $< 0.05$ (All-against-all strategy; Segata *et al.*, 2011).

Mantel test (Spearman correlation method) was employed to determine the correlation between the *I. nucleus* microbiome taxonomic structure and the oxidized PUFA products using their dissimilarity matrices across timepoints using the mantel() function in vegan package (Oksanen *et al.*, 2022), which tested whether higher dissimilarity in microbiome was associated with higher dissimilarity in metabolite profiles. Since the oysters' microbiome and metabolites were sampled from independent individuals, we averaged each microbial taxon and each metabolite concentration across replicates at each timepoints before generating a dissimilarity distance matrix between samples – Bray-Curtis (microbiome) and Euclidean (metabolites).

The GraphPad Prism software (San Diego, California, USA) was used to generate the figure for oyster's body temperatures, individual oxidized PUFA products and the 10 dominant microbe's relative abundance across the timepoints.

# Results

## *Tidal dynamics and temporal changes in environmental and body temperatures*

Oysters were regularly exposed to the air as a result of the tidal regime (Fig. 1A) and this temporal change was aligned to changes in the rock surface temperature across the day, with the highest temperature recorded at noon (45-50℃, Fig. 1A). The body temperature of the oysters varied temporally (Fig. 1B; GLM $\mathcal{X}^2_{(3)} = 1073.9$, p-value < 0.05), increasing from 32.11 ± 0.12 ℃ (mean ± SD) in the morning to 39.99 ± 0.95 ℃ (mean ± SD) at noon, after which body temperatures drop steadily to ~ 35 °C in the afternoon. Besides early-afternoon (35.4℃ ± 0.46) and late-afternoon (35.18 ℃ ± 0.46), all pairwise comparisons showed significant differences in body temperatures between timepoints.

## *Temporal assessment of oxidized PUFA products*

Individual analyses of each oxidized PUFA products revealed that only four products (i.e., 5-$F_{2t}$-IsoP, 10-$F_{4t}$-NeuroP, 13-$F_{4t}$-NeuroP, and 16-$F_{1t}$-PhytoP) significantly varied

between timepoints (Table 1, Fig. 2). There was a significant difference in the metabolites structural profile (PERMANOVA) (contributed by fifteen metabolites) between timepoints (*pseudo-F* = 2.17, p-value < 0.05; Fig. 3A), but PERMDISP indicated no significant difference in their dispersion (F-value = 0.69, p-value > 0.05; Fig. 3A). An additional PERMANOVA analysis with the four temporally-varied products showed a significant difference in the clusters between the morning metabolites profile and all the other timepoints during the emersion period (*pseudo-F* = 5.62, p-value < 0.05; Fig. 3B). Multivariate dispersion of the four oxidized PUFA products also differed between timepoints (F-value = 6.10, p-value < 0.05; Fig. 3B). With the exception of three pairwise comparisons (i.e., noon vs. early-afternoon, noon vs. late-afternoon and early-afternoon vs. late-afternoon), all the other timepoints showed significant differences in dispersion ($p < 0.05$).

## *Temporal characterization of oyster-microbiomes*

The 16S rRNA amplicon sequencing generated a total of 2,032,567 reads from 30 samples which were reduced to 1,126,884 after denoising and quality control. These reads were then used to characterize the microbial communities of *I. nucleus* across the different timepoints. Due to the low sequence counts, samples BRM3 (5612 reads) and DRM4 (7519 reads) were removed after each sample was rarefied to a sampling depth of 21,282 reads.

The ASV richness and Shannon-Wiener index of *I. nucleus* microbiome were significantly different between timepoints (ASV richness: $_{3,14)} = 3.67$; p-value < 0.05; Shannon-Wiener index: $F_{(3,14)} = 3.76$; p-value < 0.05; Fig. S2). However, no specific temporal trends were detected for all pairwise comparisons in ASV richness. Significant differences were, however, found for the Shannon-Wiener index between morning and noon timepoints. Oyster body temperature significantly influenced ASV richness and Shannon-Wiener indexes (Fig. S3). Overall, morning timepoints showed the highest alpha diversity. This diversity then drastically declined at noon, with partial recovery at the last timepoint – late-afternoon.

The top 10 most abundant microbial taxa (at the family level) associated with *I. nucleus* in a descending order were *Mycoplasmataceae, Helicobacteraceae, Spirochaetaceae, Xenococcaceae, Rhodobacteceae, Rickettsiales* unknown*, Arcobactericeae, Caldilineaceae, Alphaproteobacteria* unknown and *Saprospiraceae* (Fig. 4). These top 10 families made up on average 57.09%, 80.88%, 81.42%, and 68.20% of the overall relative abundance in morning, noon, early-afternoon, and late-afternoon, respectively. Among them, only two families (*Helicobacteraceae* and *Arcobacteraceae*) showed significant differences in the relative abundance between timepoints based on the ANCOM-BC analysis (Fig. S4; *Helicobacteraceae*: morning vs early-afternoon; *Arcobacteraceae*: morning vs noon, and morning vs early-afternoon).

LEfSe analysis identified 27 differentially abundant microbial functions (MetaCyc pathways; LDA threshold of 2.0) that characterises the microbiome at a particular timepoint (Fig. 5). The most distinctive difference in functions identified were between morning and late-afternoon timepoints, where the former showed a major enrichment in genes associated with biosynthetic pathway (and some biomolecules degradation pathways), while the latter had functions affiliated with degradation, utilization, and assimilation pathways, specifically in carbon metabolism.

Assessing the overall microbiome structure in taxonomy and functions with PERMANOVA analysis indicates no significant difference between timepoints (taxonomy: *pseudo-F* = 1.18, p-value > 0.05; function: *pseudo-F* = 1.49, p-value > 0.05 ;Fig. 6), but significant differences was detected in both of the microbial dispersion profiles (taxonomy: F-value = 3.55, p-value < 0.05; function: F-value = 3.74, p-value < 0.05 ; Fig. 6). Major differences in the taxonomic microbiome dispersion were between morning and early-afternoon, which corresponds to the pre-and post-noon period, respectively. For the functional microbiome, the pair early-afternoon-late-afternoon was the cause of the difference in

dispersion. We found no Mantel correlation was observed between the microbiome taxonomic profile and the oxidized PUFA products profile, either with the 15 (all) or 4 metabolite groups (Table 2).

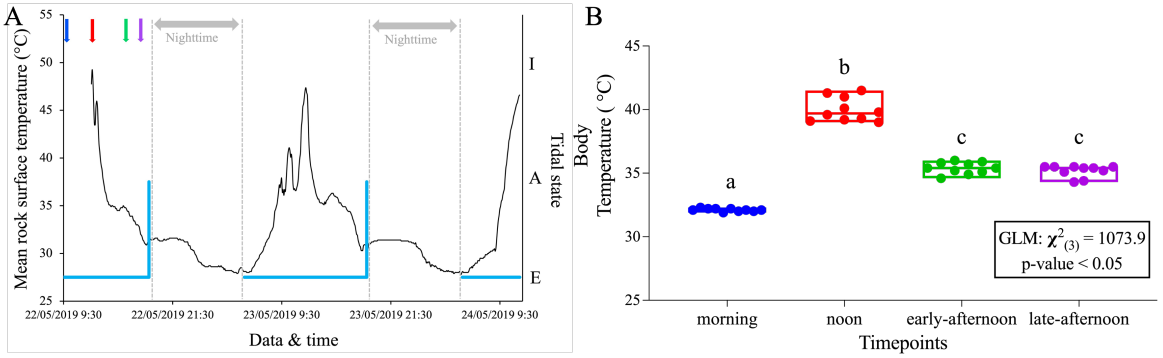


**Fig. 1. The body temperature of *Isognomon nucleus* varies across sampling timepoints within a tidal cycle.** (A) Thermal (black line) and tidal conditions (blue line) as experienced by *I. nucleus* at the study site. Thermal condition is represented by the mean rock surface temperature (averaged over 3 – 5 i-Button temperature loggers), and tidal condition during the day is categorized into three states: "E" (exposed), "A" (awash), and "I" (immersed). Coloured arrows indicate the sampling time points of *I. nucleus* (colours match to boxplot in Fig. 1B) to assess its physiological responses (i.e., biochemical dynamics) and microbiome taxonomic/functional profile (B) Boxplots showing *I. nucleus* body temperatures (n=10) across different timepoints (Centre line represent the median; box limits indicate the first and third quartiles). Statistical significance (p-value < 0.05) is indicated if the letters above each bar are different.

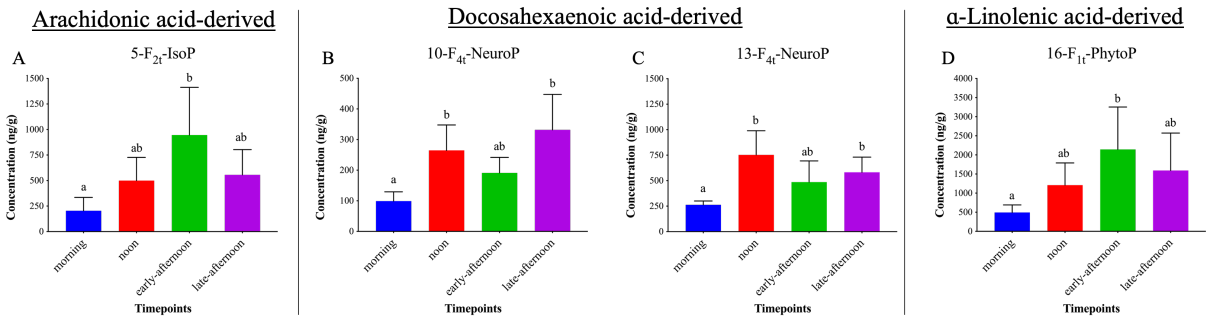


**Fig. 2. Four oxidized PUFA products exhibit variation in concentration across the emersion period.** Bar graphs showing the four oxidized PUFA products deriving from their respective PUFA (labelled at the top of each panel, across different sampling timepoints in *I. nucleus*. IsoP: isoprostane; NeuroP: neuroprostane; PhytoP: phytoprostanes. Data are presented as mean concentration and + 1 standard deviation (error bar) for each metabolite (n=5) at the given timepoints. Statistical significance (p-value < 0.05) is indicated if the letters above each bar are different.

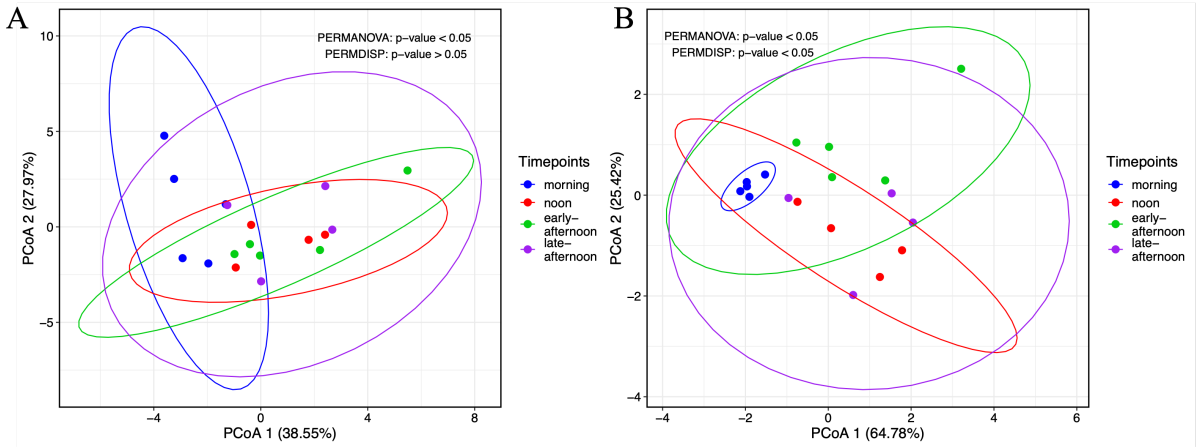


**Fig. 3. Four oxidized PUFA products exhibit variation in the sample clusters across the emersion period.** PCoA based on Euclidean distance measured between samples from different timepoints based on (A) all oxidized PUFA products (B) four oxidized PUFA products: 5-$F_{2t}$-IsoP, 10-$F_{4t}$-NeuroP, 13-$F_{4t}$-NeuroP, and 16-$F_{1t}$-PhytoP. The colours of the datapoints and ellipses (95% confidence interval of the true multivariate means) indicate their corresponding timepoints.

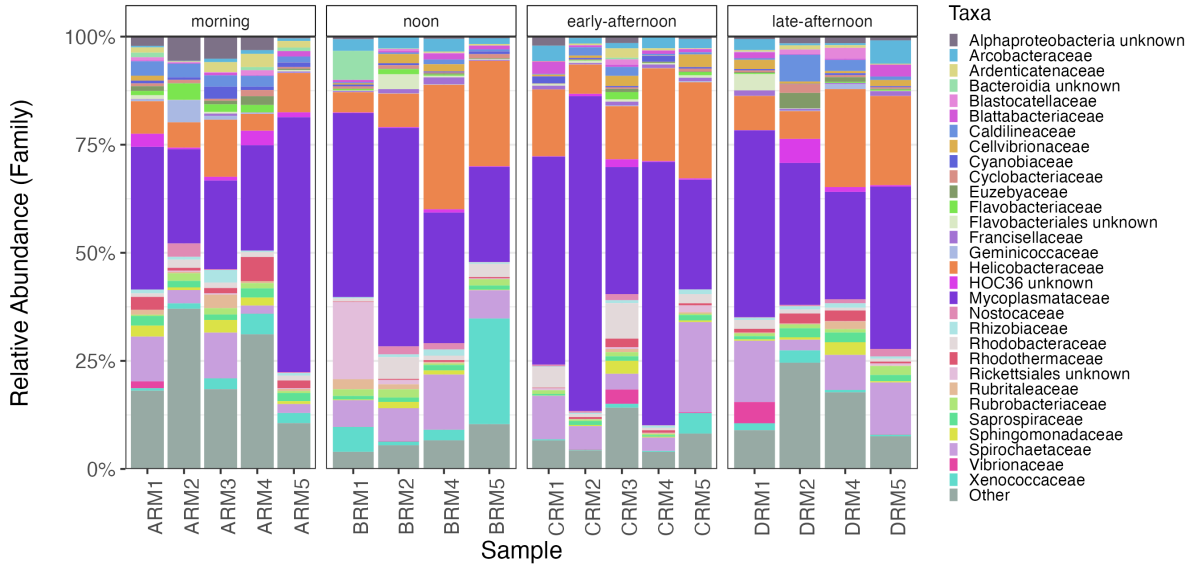


**Fig. 4. Relative abundance of top 30 most dominant microbial taxa associated with the *I. nucleus's* gut microbiome at each sampling timepoints.** ASV counts were aggregated into the family taxonomic level. Each bar represents a single individual replicate of oyster gut microbiome.

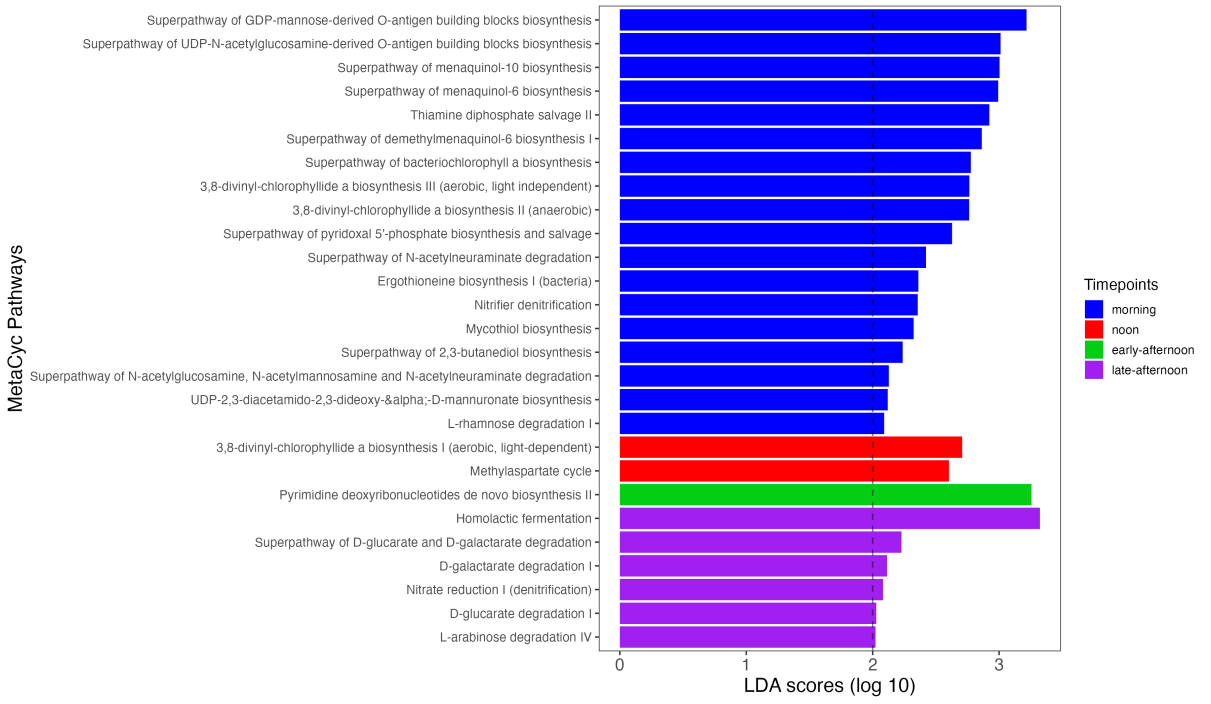


**Fig. 5. Differentially abundant microbial functions associated with a particular time point.** LEfSe analysis (LDA scores of > 2 and alpha of 0.05) showing 27 predicted functions (MetaCyc) pathways) that was identified as discriminative among the timepoints. Coloured bar represents functions that was derived from a particular timepoint. The LDA scores cut-off is depicted by the dotted lines.

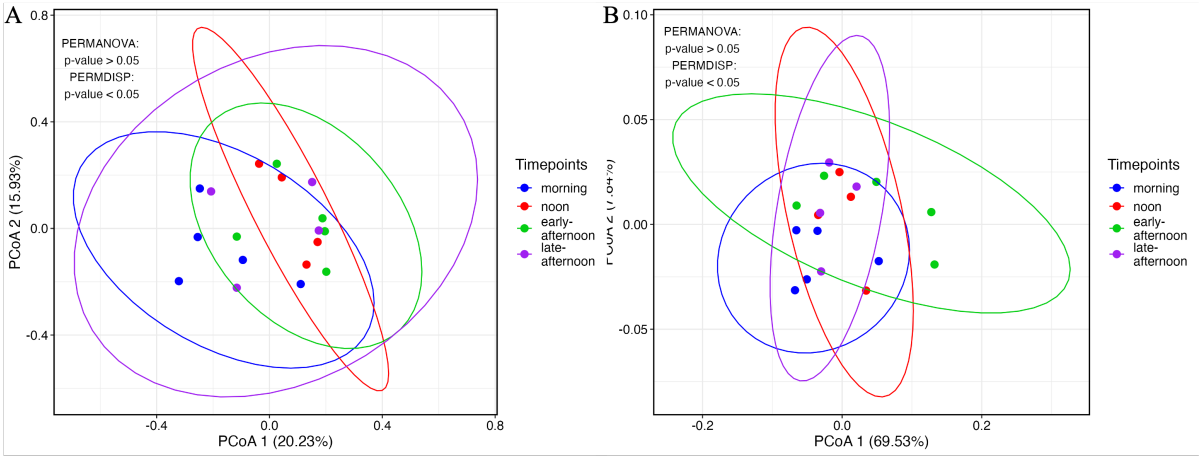


**Fig. 6. *I. nucleus*-associated microbiome taxonomic and functional structures exhibit overall stability across the emersion period.** PCoA based on the Bray-Curtis distance metric measured between samples from different timepoints, based on (A) taxonomy (ASV level) and (B) functions (MetaCyc pathways). The colours of the datapoints and ellipses (95% confidence interval of the true multivariate means) indicate their corresponding timepoints.

**Table 1**. Statistical analysis result (ANOVA or GLM with gamma distribution) testing the effect of timepoints on the concentration of each of the oxidized PUFA products.

| PUFA | Metabolite | Test Statistic | p-value |
|---|---|---|---|
| Arachidonic acid | 5-$F_{2t}$-IsoP | $F_{(3,14)} = 5.08$ | **0.04** |
| | 15-$F_{2t}$-IsoP | $F_{(3,14)} = 1.72$ | 0.21 |
| Adrenic acid | 7-$F_{2t}$-Dihomo-IsoP | $F_{(3,14)} = 3.10$ | 0.06 |
| | 17-$F_{2t}$-Dihomo-IsoP | GLM $\mathcal{X}^2_{(3)} = 0.66$ | 0.69 |
| Docosahexaenoic acid | 4-$F_{4t}$-NeuroP | $F_{(3,14)} = 3.13$ | 0.06 |
| | 10-$F_{4t}$-NeuroP | $F_{(3,14)} = 8.43$ | **< 0.01** |
| | 13-$F_{4t}$-NeuroP | GLM $\mathcal{X}^2_{(3)} = 27.46$ | **< 0.01** |
| | 20-$F_{4t}$-NeuroP | $F_{(3,14)} = 1.23$ | 0.34 |
| α-Linolenic acid | 9-$D_{1t}$-PhytoP | $F_{(3,14)} = 0.58$ | 0.64 |
| | 9-$F_{1t}$-PhytoP | GLM $\mathcal{X}^2_{(3)} = 7.92$ | 0.05 |
| | 16-$F_{1t}$-PhytoP | $F_{(3,14)} = 3.72$ | **0.04** |
| | 16-$B_{1t}$-PhytoP | GLM $\mathcal{X}^2_{(3)} = 6.66$ | 0.08 |
| Eicosapentaenoic acid | 5-$F_{3t}$-IsoP | $F_{(3,14)} = 2.49$ | 0.10 |
| | 15-$F_{3t}$-IsoP | GLM $\mathcal{X}^2_{(3)} = 0.32$ | 0.32 |
| | 8-$F_{3t}$-IsoP | $F_{(3,14)} = 0.81$ | 0.51 |

**Table 2**. Mantel's spearman's rank correlation (r) and p-value to investigate the association between the *I. nucleus* microbiome taxonomic structure (mean abundance of each taxon across all timepoints) and oxidized PUFA products profile (mean concentration across timepoints). The number of permutations performed was 23(maximum possible).

| Association with microbiome taxonomic structure | Mantel's r | p-value |
|---|---|---|
| oxidized PUFA products (all) | 0.77 | 0.21 |
| oxidized PUFA products (Four)* | 0.54 | 0.25 |

*The four metabolites were: 5-$F_{2t}$-IsoP, 10-$F_{4t}$-NeuroP, 13-$F_{4t}$-NeuroP, and 16-$F_{1t}$-PhytoP

# Discussion

Organisms living on the intertidal rocky shore regularly experience drastic changes in environmental temperature (Somero, 2002; Stillman, 2002; Harley, 2008). For many sessile ectotherms, this represents a physiological challenge due to their inability to escape from heat stress (e.g. seeking thermal refuge) and so, they rely on various intrinsic (e.g., metabolic and physiological plasticity) and extrinsic (e.g., host-associated microbiome; still underexplored) mechanisms to cope with temperature fluctuations (Lathlean *et al.*, 2014; Giomi *et al.*, 2016; Bang *et al.*, 2018). As with other ectotherms, the body temperature of the high-supratidal zone inhabiting oyster, *Isognomon nucleus* was highly influenced by changes in ambient temperatures throughout the day. Such changes are known to induce physiological stress and metabolic depression (Hui *et al.*, 2020), with the associated oxidative stress (Hermes-Lima *et al.*, 2015). Here, linked to these physiological conditions, we found adjustments in four major non-enzymatic oxidized PUFA products (i.e., 5-$F_{2t}$-IsoP, 10-$F_{4t}$-NeuroP, 13-$F_{4t}$-NeuroP, and 16-$F_{1t}$-PhytoP) that reflect temporal variation in the oxidative stress experienced by the oysters. Contrary, based on beta-diversity analysis that assess all samples simultaneously across timepoints, no clear temporal change in the structure and/or function of the gut microbiome were detected. This suggests that the oyster gut microbiome is temporally stable and insensitive to extreme high thermal conditions (> 40ºC in body temperature) at noon that are

physiologically stressful to the oyster host. The differences in the host and microbiome sensitivity to external changes was further supported in the lack of temporal correlation between the intrinsic (biochemical profile) and extrinsic (microbiome taxonomic structure) mechanisms. In summary, the microbiome stability may be important for the overall homeostasis of the oysters, contributing to their thermal tolerance and survival in the challenging tropical intertidal rocky environment.

### *The intrinsic mechanism underpinning oysters' adaptive response to temporal environmental changes*

For high-supratidal zone inhabiting ectotherms, metabolic depression is an adaptive response that allows them to cope with extreme high and stressful thermal conditions (Sokolova and Pörtner, 2001; Marshall *et al.*, 2011). In a laboratory setting, Hui et al. (2020) demonstrated that the oyster *I. nucleus* consistently enters into metabolic depression (i.e., measured by heart rate) when body temperature approaches ~ 37℃ (a value that is regularly surpassed on daily basis at around noon on tropical rocky shores). Our data indicates that the oysters could have enterred a state of metabolic depression when exposed by the tide during noon time and resume their metabolism when body temperatures lower in late afternoon/evening, or when they are re-immersed

Intertidal bivalves are known to also display intermittent gaping behaviour during periods of aerial exposure as a way to enhance oxygen intake and evaporative cooling, particularly when experiencing thermal stress (Lent, 1969; Mcmahon, 1988; Nicastro *et al.*, 2010). In our study, all individuals shut their valves and no intermittent gaping behaviour was observed either during the high thermal stress or the recovering period (Hui, T.Y., unpublished data). Therefore, oxygen depletion in addition to thermal stress in the oysters particularly during noon time could contribute to the intense oysters' metabolic demand of which, metabolic depression is likely to be a key strategy for survival during the emersion period.

548 There were four metabolites (i.e., 5-$F_{2t}$-IsoP (Isoprostane), 10-$F_{4t}$-NeuroP
549 (Neuroprostane), 13-$F_{4t}$-NeuroP (Neuroprostane), and 16-$F_{1t}$-PhytoP (Phytoprostane)) that
550 showed visible temporal patterns that may be associated with their metabolic regulation. Such
551 patterns may be linked to the sensitivity of the metabolites to ROS changes in the oyster.
552 Elevation of 5-$F_{2t}$-IsoP, 10-$F_{4t}$-NeuroP, and 13-$F_{4t}$-NeuroP during noon, and 16-$F_{1t}$-PhytoP at
553 post-noon timepoints, clearly indicates that oysters experienced a rise in the ROS level, a signal
554 of oxidative stress (Hermes-Lima and Zenteno-Savín, 2002; Storey and Storey, 2004;
555 Sussarellu *et al.*, 2012; Welker *et al.*, 2013; Galano *et al.*, 2017). This could be caused by an
556 increase in metabolic demand and/or hypoxia (when individuals shut their valves and show no
557 gaping behaviour). In our study, the high levels of 16-$F_{1t}$-PhytoP (Phytoprostane) metabolites
558 as compared to other three oxidized PUFA products in the *I. nucleus,* imply that the PUFA
559 ALA could also be the predominant fatty acid in alleviating oxidative stress in this oyster.
560 Further analysis with the overall structural profile with the four ROS-sensitive oxidized
561 PUFA products showed a clear temporal variation and inter-individual variation in *I. nucleus*.
562 The large inter-individual variation in the oxidized PUFA products profile at noon/afternoon
563 relative to morning timepoint might be related to the thermal and oxidative stress conditions
564 experienced by the oysters during those periods of elevated temperatures. This variability
565 suggests inter-individual differences in physiological plasticity, regulation, and sensitivities to
566 environmental stress. The result here also indicates that the polyunsaturated fatty acids (ARA,
567 DHA, and ALA) from which these four oxidized PUFA products were derived, may play a key
568 role as lipid metabolites that help to resolve inflammation and oxidative stress for the oysters
569 to return to homeostasis (Roy *et al.*, 2017; Lee *et al.*, 2020). It is important to highlight here
570 that the current understanding regarding the thermal-physiological roles of high PUFA ALA or
571 the oxidized PUFA products in *I. nucleus* is still limited and that our interpretations are
572 speculative and idiosyncratic to the specific animals and population studied. Moreover, our

assessment was based on the observation and analysis that are known in clinical research and we remained carefully and strictly conservative in our discussion to just focus on the association between these products and the host oxidative stress level. Future studies would be dedicated toward elucidating the role of these molecules that may be essential to their host physiology and metabolism.

### *The extrinsic mechanism underpinning the oysters' response to temporal environmental changes*

Host-associated microbiome diversity, structure, and functions are considered as important components of animal adaptation and acclimation to environmental change (Foster *et al.*, 2017; Bang *et al.*, 2018; Voolstra and Ziegler, 2020). Alterations in microbiome diversity can be associated with the direct influence of the host's physiology and/or with host-independent environmental effects (Shiu *et al.*, 2017; Li *et al.*, 2018, 2022; Muñoz *et al.*, 2019). In our study, the composition and diversity (ASV richness and Shannon diversity) of the oyster gut-associated microbiome varied with time which coincided with variation in the oyster's body temperature, suggesting that the thermal condition experienced by the host may modulate the microbial alpha diversity via either direct/indirect physio-biochemical influences (Sorek *et al.*, 2014; Pita *et al.*, 2018; Liu *et al.*, 2023). In the morning, the oyster's gut had a significantly more diverse microbiome diversity, which may be linked to the less thermally stressed host (Hui *et al.*, 2020), and/or to the filter-feeding activities before being exposed by the receding tide (Parris *et al.*, 2019). However, based on the Shannon alpha diversity, at early post-noon condition, a major decline in diversity was observed, which may be associated with the thermal physiological stress experienced by the host (body temperature is within the metabolic depression range; Hui *et al.*, 2020) and oxidative stress (indicated by the rise in the two oxidized PUFA products at noon and two at early post-noon condition). This decline in diversity is also a common pattern seen in many marine organisms under physiological stress (Green and Barnes,

2010; Li *et al.*, 2018; Hartman *et al.*, 2020). For example, Lokmer & Wegner (2015) showed that acute thermal stress and/or infection caused a marked decline in the alpha diversity of the microbiome in the oyster *Crassostrea gigas*. In another study by Li et al. (2018) observed an overall decrease in the gut microbial alpha diversity associated with the mussel, *Mytilus coruscus*, after exposing to higher temperature. Such observation offer support to our result where the relatively higher temperature at noon may have driven the decline in the oyster-associated microbial diversity.

Whilst the temporal changes exhibited by the *I. nucleus* microbiome and their association with changes in the oysters' body temperatures suggest that the microbiome composition may be actively regulated by the host, differential sensitivities of certain bacterial taxa to external environmental changes may also be an important mechanism driving the temporal variation in the microbiome composition. *Arcobacteraceae* and *Helicobacteraceae* are the only two dominant family-level microbial taxa associated with the temporal thermal/oxidative stress variation of the host. In particular, there was an elevated relative abundance of these two bacteria groups at noon and/or at the afternoon timepoints, which may suggest that their abundances during these periods were promoted by specific host/environmental conditions, facilitating their growth probably by reducing competition (Garren *et al.*, 2016; Shaver *et al.*, 2017; Sharp and Foster, 2022). *Arcobacteraceae* is a group of common opportunistic bacteria found in marine bivalves and is known to be associated with disease-causing bacteria such as *Vibrio* (Lokmer and Wegner, 2015; de Lorgeril *et al.*, 2018). In many studies, the elevation of the *Arcobacteraceae* has been associated with the thermal stress condition experienced by the host (Lokmer and Wegner, 2015; Shiu *et al.*, 2017; Neu *et al.*, 2021). Members of *Arcobacteraceae* are also known to be microaerophilic as they tend to grow better under a low-oxygen environment (Vandamme and De Ley, 1991). This may explain the dominant presence of *Arcobacteraceae* within the oysters' microbiome due to the prevailing

hypoxic and thermally stressful conditions as experienced by the oyster hosts during emersion. Similarly, the presence and abundance *Helicobacteraceae* can be associated to oxygen levels in the marine environment. For instance, certain members of this family are capable of oxidising sulfide, and thus, they might contribute with a detoxification function to the oyster host (Kodama and Watanabe, 2004; Nakagawa *et al.*, 2017; Neu *et al.*, 2021). The accumulation of sulfide can be detrimental or lethal to marine bivalves (Le Moullac *et al.*, 2008), and it is typically associated with hypoxic stress (Le Moullac *et al.*, 2008; Pal *et al.*, 2018). Such stress is hypothesised to occur in *I. nucleus* during aerial exposure, as no intermittent gaping behaviour was detected. When oxygen is low, sulfide production is promoted by the activity of hydrogen sulfide-producing bacteria such as *Desulfobacterota* members (Flannigan *et al.*, 2011; present in the I. nucleus; Dordević *et al.*, 2021; Pimentel *et al.*, 2021). It is unclear, however, the extent to which the dynamics in the abundance of sulfide-producing bacteria and *Helicobacteraceae* members (with potential detoxification role), are functionally interconnected. While this seems likely, we are unaware of any study exploring this functional link, and it would be important to investigate such species' interaction and its effects on the physiology and fitness of the host.

Variation in the microbiome functional activity is commonly associated with the functional changes occurring within the host (e.g., dietary changes; Mekuchi *et al.*, 2018; Masasa *et al.*, 2023) and/or in the external environment (e.g., temperature; Brothers *et al.*, 2018; Li *et al.*, 2022). Our study is in-line with this, in showing that there were several enriched functions that vary through time, potentially attributed to either one or both of those two factors. Specifically, in the morning timepoints, we detected a major proportion of predicted microbiome function in biosynthetic pathways associated with carbohydrate, cofactor, carrier, vitamin and secondary metabolites biosynthesis. This suggested that, in the morning, the host gut had a considerable dietary resources for the building of these organic/inorganic molecules

649 in microbes to support cellular maintenance and growth and/or actively contributing to host
650 nutritional metabolism (David *et al.*, 2014; Maurice *et al.*, 2015; Dubé *et al.*, 2019). On contrary,
651 post-noon conditions were significantly dominated by compound/molecular degradation
652 pathways associated with carbon metabolism. This makes sense since in the post-noon
653 conditions (post-heat stress), the host are likely in a "recovery" that could incur a high energetic
654 requirement for various cellular and physiological repair and maintenance purposes (Storey and
655 Storey, 2004; Sokolova *et al.*, 2011). The breakdown of these carbon compounds by the
656 microbes can provide as an energy source to meeting the metabolic demand in the host and
657 microbes (Flint *et al.*, 2012; Tremaroli and Bäckhed, 2012; Den Besten *et al.*, 2013). However,
658 it is unclear if these predicted microbial functional enrichments are directly contributing to the
659 host dietary metabolism (e..g., nutrient absorption; English *et al.*, 2023) or simply fulfilment of
660 need for the microbes themselves (host-independent) to cope and survive to the prevailing
661 conditions (i.e., host and/or external environmental influence).

662 Host tolerance and resilience to environmental stress are known to be conditioned by
663 the stability/flexibility of its associated microbiome. Despite the changes in the alpha diversity
664 and relative abundance of some of the most abundant bacteria (family level) in *I. nucleus*, the
665 beta analysis that assesses the structural microbiome profiles among samples simultaneously
666 showed no changes in their taxonomy and function throughout the day (emersion period). This
667 suggest that despite experiencing high thermal stress at noon (Hui *et al.*, 2020), there is an
668 overall stability in the microbiome composition and structure. Such stability could be
669 potentially explained by the ability of the host to control/regulate the microbiome during a
670 disturbance event (Sharp *et al.*, 2017; Pita *et al.*, 2018; Rocca *et al.*, 2019; Rädecker *et al.*,
671 2022). Alternatively, the stability of the microbiome may reflect its own resilience (or lower
672 sensitivity), rather than the host control/regulation, to changing and stressful environments
673 (Soen, 2014). This characteristic could be essential for host tolerance and acclimation to

environmental challenges such as thermal stress. For example, Santoro et al. (2021) demonstrated that the stability of inoculated "beneficial microorganisms" in the coral *Mussismilia hispida* provided a thermal protection effect, reducing heat stress and preventing the associated mortality (40% increase in the survival rate) of the hosts. Contrary, disruptions in the microbiome structure and function can lead to a weakened thermal tolerance and performance of the host, and a decrease in survival rate under prolonged heat stress condition, particularly in early ontogenetic stages such as in the tadpoles of the green frog *Lithobates clamitans* (Fontaine *et al.*, 2022). Regardless whether it is host control or microbiome structural resilience (independent of the host influence), the temporal stability in the microbiome structure and function observed suggest that it may contribute to the survival of *I. nucleus* in the thermally extreme tropical intertidal environment (Bang *et al.*, 2018; Aktipis and Beltran, 2021).

### *No correlation between microbiome structure and oxidized PUFA products profile*

Over the decades, many studies have documented the role and action of PUFA (e.g., as probiotics) in modulating dynamics in the gut microbiome of different animals (Huyben *et al.*, 2020; Fu *et al.*, 2021; Lau *et al.*, 2022; Ma *et al.*, 2022). Hence, it is expected that stress-driven changes in these biochemicals and their by-products would influence the oyster gut microbiome. However, we found no correlation between the oxidized PUFA products (averaged across all tissues) and the gut microbiome taxonomic structure in *I. nucleus*, despite the temporal and inter-individual variation in the oxidized PUFA products profile across the emersion period. The lack of association between the microbial and oxidized PUFA products profiles of *I. nucleus*, suggests two possibilities that are not mutually exclusive. Firstly, as mentioned previously, physiological/biochemical and microbiome profiles may have different sensitivities to changes in environmental conditions. Secondly, such microbiome profiles and biochemical responses may not show strong variation and/or alignment because of local adaptation. Here,

the thermal window and oxygen levels experienced by the oysters, although extreme for many ectotherms, can be considered within the tolerance range of the species. Several studies have shown that the microbiome-metabolites correlation is detectable only under severe post-disturbance events and unhealthy host conditions (Nguyen *et al.*, 2021; Pimentel *et al.*, 2021; Walke *et al.*, 2021; Mallott *et al.*, 2022), which go beyond tolerance levels. Thus, in this study, oysters may be in a condition where stress is within the tolerance range, and thus no correlation can be observed between these two components (i.e., host biochemical profile and microbiome structure). Future studies aiming to explore the functional regulation and interplay between intrinsic and extrinsic mechanisms in ectotherms living in the thermally extreme and fluctuating environment like in this study, the intertidal rocky shore, require the assessment of both components when animals are closer to, or surpass their physiological tolerance limits at sublethal levels.

### *Study limitations*

While our findings are noteworthy, here we discuss some study limitations and potential recommendations to address them. First, temperature-modulated dynamics in host-associated microbial communities and biochemical profiles across the day lacked temporal replication. Although the selected timepoints are eco-physiologically relevant for the oysters, the consistency and repeatability of the trends observed can only be assessed by sampling at different and independent days (i.e., two or more non-consecutive days). Second, the timepoints selected, although extreme for most ectotherms on Earth, fell within a thermal window that represents acute low physiological stress to the oysters. Major and divergent differences in extrinsic and intrinsic responses might potentially be detected under acute high or chronic physiological stress when body temperatures reach the maximum temperature documented for this species 50-52ºC in the field (Fig. 1). Third, the existence of an interacting drivers that may

influence the microbiome altogether, such as, temperature, hypoxic condition (no gaping in the oyster) and the emersion duration. This makes our study difficult to distinguish the influence of a sole driver in the field. Fourth, the oyster microbiome can exhibit tissue-specific profiles associated to functional differences (Dubé *et al.*, 2019). Here, our focus was the gut microbiome as its captures a large diverse microbial sets associated with their host (King *et al.*, 2012; Pierce and Ward, 2018; Dubé *et al.*, 2019), and several documented findings showing their strong and direct signal of their host physiological states (Li *et al.*, 2018; Pierce and Evan, 2019; Fassarella *et al.*, 2021; Stevick *et al.*, 2021). However, other tissues such as the haemolymph or the gills of the oysters can provide complementary information regarding the interaction between microbial communities and their host under environmental stress (Lokmer and Wegner, 2015; Scanes *et al.*, 2021). Despite these limitations, our study provides for the first-time empirical evidence of the intrinsic and extrinsic mechanisms underpinning the temperature tolerances and ecological success of tropical high-supratidal zone inhabiting ectotherms. Future studies can integrate our recommendations to provide more robust and independent assessments of temporal dynamics in temperature-modulated functional responses of ectotherms in extreme environments.

# Conclusion

Intrinsic (e.g., non-enzymatic oxidized PUFA products) and extrinsic (e.g., microbiome profile) mechanisms linked to the ecophysiology and tolerance/sensitivity of the oyster *Isognomon nucleus*, showed temporal variation indicative of thermal and oxidative stress. Such trend showed a temporal association with the environmental and body temperatures during the tidal cycle where oysters were fully emersed. Although the microbial alpha diversity in the oyster gut varied along this temporal and environmental cycle, no major changes were detected in the overall structure and function of the associated microbial communities. This microbiome

stability along periods of extreme high temperature and oxygen deprivation, could be explained by the potential regulatory influence of the host (consistent with the Anna Karenina Principle) and/or the insensitivity of these microorganisms to the environmental changes experienced in the tropical rocky shores. When assessing both the intrinsic and extrinsic mechanisms together, we found no clear correlation between the oxidized PUFA products profile and the microbiome profile. However, some specific bacteria groups (i.e., *Helicobacteraceae* and *Arcobacteraceae*) increased during stressful periods, potentially linked to the lower oxygen availability within the oysters due to the lack of gaping behaviour when emersed. These microorganisms may provide important functions for the resilience and stability of the overall microbial community, as well as for the health and survival of the oyster host in the thermally challenging rocky intertidal environment. The overall microbiome stability can avoid dysbiosis and contribute to the intrinsic adaptive adjustment of oyster physiology and biochemistry. To our best knowledge, this is the first study to report the use of non-enzymatic oxidized PUFA products as a proxy for oxidative stress levels in intertidal animals and profiling short-term dynamics of the host-associated microbiome in an intertidal environment. Future investigations should aim to explore the interplay between these biomolecules and microbial patterns when stressful environmental conditions are unpredictable and beyond tolerance windows of the hosts. Moreover, it is important to understand whether these functional links between intrinsic and extrinsic mechanisms are modulated by local adaptation and can be shared among other intertidal organisms.

# Competing interests

The authors declare no competing or financial interests

## Author Contributions

JDGE and BSA conceived the idea and designed the work. BSA carried out most of the work: data collection, sample processing, statistical analyses, and data presentation. AWTC, HTY GAW, and MG were involved in sample and environmental data collection. LKS performed the oxidized PUFA products extraction and processing. TD supplied the in-house synthesised oxidized lipids standards for PUFA metabolites quantification. JTY and TD were involved in analysing the metabolite data. BSA led the manuscript writing with continuous feedback from JDGE. All authors provided feedback on the final version of this work, and accepted responsibility for the entire content of this manuscript.


## Acknowledgement

We would like to thank The Swire Group of Companies, especially Ms. Tina Chan and Cathay Pacific staff for arranging air transportation of equipment to and from Thailand from Hong Kong

## Funding

BA and JDGE were supported by the Research Grants Council (GRF 17113221) of Hong Kong.


## Data availability

All raw data, and scripts will be made available once published.

# References


Ahmed, H.I., Herrera, M., Liew, Y.J., and Aranda, M. (2019) Long-term temperature stress in the coral model Aiptasia supports the "Anna Karenina Principle" for bacterial microbiomes. *Front Microbiol* **10**: 975.

Aktipis, A. and Beltran, D.G. (2021) Can some microbes promote host stress and benefit evolutionarily from this strategy? *BioEssays* **43**: 1–11.

Alberdi, A., Aizpurua, O., Bohmann, K., Zepeda-Mendoza, M.L., and Gilbert, M.T.P. (2016) Do vertebrate gut metagenomes confer rapid ecological adaptation? *Trends Ecol Evol* **31**: 689–699.

Apprill, A. (2017) Marine animal microbiomes: Toward understanding host-microbiome interactions in a changing ocean. *Front Mar Sci* **4**: 222.

Bang, C., Dagan, T., Deines, P., Dubilier, N., Duschl, W.J., Fraune, S., et al. (2018) Metaorganisms in extreme environments: do microbes play a role in organismal adaptation? *Zoology* **127**: 1–19.

Basu, S. (2010) Fatty acid oxidation and isoprostanes: Oxidative strain and oxidative stress. *Prostaglandins Leukot Essent Fat Acids* **82**: 219–225.

van den Berg, R.A., Hoefsloot, H.C.J., Westerhuis, J.A., Smilde, A.K., and van der Werf, M.J. (2006) Centering, scaling, and transformations: Improving the biological information content of metabolomics data. *BMC Genomics* **7**: 1–15.

Den Besten, G., Van Eunen, K., Groen, A.K., Venema, K., Reijngoud, D.J., and Bakker, B.M. (2013) The role of short-chain fatty acids in the interplay between diet, gut microbiota, and host energy metabolism. *J Lipid Res* **54**: 2325–2340.

Birben, E., Sahiner, U.M., Sackesen, C., Erzurum, S., and Kalayci, O. (2012) Oxidative stress and antioxidant defense. *World Allergy Organ J* **5**: 9–19.

Bolyen, E., Rideout, J.R., Dillon, M.R., Bokulich, N.A., Abnet, C.C., Al-Ghalith, G.A., et al. (2019) Reproducible, interactive, scalable and extensible microbiome data science using QIIME 2. *Nat Biotechnol* **37**: 852–857.

Brothers, C.J., Pol, W.J. Van Der, Morrow, C.D., Hakim, J.A., Koo, Hyunmin, Mcclintock, J.B., et al. (2018) Ocean warming alters predicted microbiome functionality in a common sea urchin. *Proc R Soc B Biol Sci* **285**:.

Callahan, B.J., McMurdie, P.J., and Holmes, S.P. (2017) Exact sequence variants should replace operational taxonomic units in marker-gene data analysis. *ISME J* **11**: 2639–2643.

Callahan, B.J., McMurdie, P.J., Rosen, M.J., Han, A.W., Johnson, A.J.A., and Holmes, S.P. (2016) DADA2: High-resolution sample inference from Illumina amplicon data. *Nat Methods* **13**: 581–583.

Carey, H. V. and Duddleston, K.N. (2014) Animal-microbial symbioses in changing environments. *J Therm Biol* **44**: 78–84.

Chow, C.Y. (2004) Foraging behaviour of Thais clavigera: The interplay of environmental variation and predator behaviour on sheltered rocky shores.

David, L.A., Maurice, C.F., Carmody, R.N., Gootenberg, D.B., Button, J.E., Wolfe, B.E., et al. (2014) Diet rapidly and reproducibly alters the human gut microbiome. *Nature* **505**: 559–563.

Díaz-Almeyda, E.M., Ryba, T., Ohdera, A.H., Collins, S.M., Shafer, N., Link, C., et al. (2022) Thermal stress has minimal effects on bacterial communities of thermotolerant *Symbiodinium* cultures. *Front Ecol Evol* **10**: 764086.

Dordević, D., Jančíková, S., Vítězová, M., and Kushkevych, I. (2021) Hydrogen sulfide toxicity in the gut environment: Meta-analysis of sulfate-reducing and lactic acid bacteria in inflammatory processes. *J Adv Res* **27**: 55–69.

847 Douglas, G.M., Maffei, V.J., Zaneveld, J.R., Yurgel, S.N., Brown, J.R., Taylor, C.M., et al.
848 (2020) PICRUSt2 for prediction of metagenome functions. *Nat Biotechnol* **38**: 669–673.
849 Dubé, C.E., Ky, C.L., and Planes, S. (2019) Microbiome of the black-lipped pearl oyster
850 *Pinctada margaritifera*, a multi-tissue description with functional profiling. *Front*
851 *Microbiol* **10**: 1548.
852 Dupuy, A., Le Faouder, P., Vigor, C., Oger, C., Galano, J.M., Dray, C., et al. (2016)
853 Simultaneous quantitative profiling of 20 isoprostanoids from omega-3 and omega-6
854 polyunsaturated fatty acids by LC-MS/MS in various biological samples. *Anal Chim*
855 *Acta* **921**: 46–58.
856 Durand, T., Bultel-Poncé, V., Guy, A., Berger, S., Mueller, M.J., and Galano, J.M. (2009)
857 New bioactive oxylipins formed by non-enzymatic free-radical-catalyzed pathways: The
858 phytoprostanes. *Lipids* **44**: 875–888.
859 English, M.K., Langdon, C.J., Schubiger, C.B., and Mueller, R.S. (2023) Dominant bacterial
860 taxa drive microbiome differences of juvenile Pacific oysters of the same age and
861 variable sizes. 1–12.
862 Epstein, H.E., Torda, G., and van Oppen, M.J.H. (2019) Relative stability of the *Pocillopora*
863 *acuta* microbiome throughout a thermal stress event. *Coral Reefs* **38**: 373–386.
864 Fadhlaoui, M. and Lavoie, I. (2021) Effects of temperature and glyphosate on fatty acid
865 composition, antioxidant capacity, and lipid peroxidation in the gastropod lymneae sp.
866 *Water (Switzerland)* **13**:.
867 Fan, L., Liu, M., Simister, R., Webster, N.S., and Thomas, T. (2013) Marine microbial
868 symbiosis heats up: the phylogenetic and functional response of a sponge holobiont to
869 thermal stress. *ISME J* **7**: 991–1002.
870 Fassarella, M., Blaak, E.E., Penders, J., Nauta, A., Smidt, H., and Zoetendal, E.G. (2021) Gut
871 microbiome stability and resilience: Elucidating the response to perturbations in order to
872 modulate gut health. *Gut* **70**: 595–605.
873 Feng, J., Zhang, L., Tang, X., Xia, X., Hu, W., and Zhou, P. (2021) Season and geography
874 induced variation in sea cucumber (*Stichopus japonicus*) nutritional composition and gut
875 microbiota. *J Food Compos Anal* **101**: 103838.
876 Flannigan, K.L., McCoy, K.D., and Wallace, J.L. (2011) Eukaryotic and prokaryotic
877 contributions to colonic hydrogen sulfide synthesis. *Am J Physiol - Gastrointest Liver*
878 *Physiol* **301**: 188–193.
879 Flint, H.J., Scott, K.P., Duncan, S.H., Louis, P., and Forano, E. (2012) Microbial degradation
880 of complex carbohydrates in the gut. *Gut Microbes* **3**:.
881 Folch, J., Lees, M., and Sloane Stanley, G.H. (1957) A simple method for the isolation and
882 purification of total lipides from animal tissues. *J Biol Chem* **226**: 497–509.
883 Fontaine, S.S. and Kohl, K.D. (2023) The microbiome buffers tadpole hosts from heat stress :
884 a hologenomic approach to understand host-microbe interactions under warming. *J ofp*
885 *Exp Biol* **226**:.
886 Fontaine, S.S., Mineo, P.M., and Kohl, K.D. (2022) Experimental manipulation of microbiota
887 reduces host thermal tolerance and fitness under heat stress in a vertebrate ectotherm.
888 *Nat Ecol Evol* **6**: 405–417.
889 Foster, K.R., Schluter, J., Coyte, K.Z., and Rakoff-Nahoum, S. (2017) The evolution of the
890 host microbiome as an ecosystem on a leash. *Nature* **548**: 43–51.
891 Fox, J. and Weisberg, S. (2019) An R Companion to Applied Regression.
892 Freire, C.A., Welker, A.F., Storey, J.M., Storey, K.B., and Hermes-lima, M. (2011) Oxidative
893 Stress in Estuarine and Intertidal Environments (Temperate and Tropical). In *Oxidative*
894 *Stress in Aquatic Ecosystems*. Abele, D., Pablo, J., Vázquez-Medina, and Zenteno-Savín,
895 T. (eds). Blackwell Publishing Ltd, pp. 41–57.
896 Fu, Y., Wang, Y., Gao, H., Li, D., Jiang, R., Ge, L., et al. (2021) Associations among Dietary

Omega-3 Polyunsaturated Fatty Acids, the Gut Microbiota, and Intestinal Immunity. *Mediators Inflamm* **2021**:.
Galano, J.M., Lee, Y.Y., Oger, C., Vigor, C., Vercauteren, J., Durand, T., et al. (2017) Isoprostanes, neuroprostanes and phytoprostanes: An overview of 25 years of research in chemistry and biology. *Prog Lipid Res* **68**: 83–108.
Garren, M., Son, K., Tout, J., Seymour, J.R., and Stocker, R. (2016) Temperature-induced behavioral switches in a bacterial coral pathogen. *ISME J* **10**: 1363–1372.
Garrity, S.D. (1984) Some adaptations of gastropods to physical stress on a tropical rocky shore. *Ecology* **65**: 559–574.
Giomi, F., Mandaglio, C., Ganmanee, M., Han, G.D., Dong, Y., Williams, G.A., and Sara, G. (2016) The importance of thermal history: Costs and benefits of heat exposure in a tropical, rocky shore oyster. *J Exp Biol* **219**: 686–694.
Green, T.J. and Barnes, A.C. (2010) Bacterial diversity of the digestive gland of Sydney rock oysters, *Saccostrea glomerata* infected with the paramyxean parasite, *Marteilia sydneyi*. *J Appl Microbiol* **109**: 613–622.
Harley, C.D.G. (2008) Tidal dynamics, topographic orientation, and temperature-mediated mass mortalities on rocky shores. *Mar Ecol Prog Ser* **371**: 37–46.
Hartman, L.M., van Oppen, M.J.H., and Blackall, L.L. (2020) The effect of thermal stress on the bacterial microbiome of *Exaiptasia diaphana*. *Microorganisms* **8**: 1–18.
Helmuth, B. and Hofmann, G.E. (2001) Microhabitats, thermal heterogeneity, and patterns of physiological stress in the rocky intertidal zone. *Biol Bull* **201**: 374–384.
Herlemann, D.P.R., Labrenz, M., Jürgens, K., Bertilsson, S., Waniek, J.J., and Andersson, A.F. (2011) Transitions in bacterial communities along the 2000 km salinity gradient of the Baltic Sea. *ISME J* **5**: 1571–1579.
Hermes-Lima, M., Moreira, D.C., Rivera-Ingraham, G.A., Giraud-Billoud, M., Genaro-Mattos, T.C., and Campos, É.G. (2015) Preparation for oxidative stress under hypoxia and metabolic depression: Revisiting the proposal two decades later. *Free Radic Biol Med* **89**: 1122–1143.
Hermes-Lima, M. and Zenteno-Savín, T. (2002) Animal response to drastic changes in oxygen availability and physiological oxidative stress. *Comp Biochem Physiol - C Toxicol Pharmacol* **133**: 537–556.
Herrera, M., Klein, S.G., Schmidt-Roach, S., Campana, S., Cziesielski, M.J., Chen, J.E., et al. (2020) Unfamiliar partnerships limit cnidarian holobiont acclimation to warming. *Glob Chang Biol* **26**: 5539–5553.
Hui, T.Y., Dong, Y., Han, G.D., Lau, S.L.Y., Cheng, M.C.F., Meepoka, C., et al. (2020) Timing metabolic depression: Predicting thermal stress in extreme intertidal environments. *Am Nat* **196**: 501–511.
Huyben, D., Roehe, B.K., Bekaert, M., Ruyter, B., and Glencross, B. (2020) Dietary lipid:Protein ratio and n-3 long-chain polyunsaturated fatty acids alters the gut microbiome of Atlantic salmon under hypoxic and normoxic conditions. *Front Microbiol* **11**: 589898.
Jaramillo, A. and Castañeda, L.E. (2021) Gut Microbiota of Drosophila subobscura Contributes to Its Heat Tolerance and Is Sensitive to Transient Thermal Stress. *Front Microbiol* **12**: 1–13.
Kandlikar, G.S., Gold, Z.J., Cowen, M.C., Meyer, R.S., Freise, A.C., Kraft, N.J.B., et al. (2018) Ranacapa: An R package and shiny web app to explore environmental DNA data with exploratory statistics and interactive visualizations. *F1000Research* **7**: 1–19.
Kers, J.G. and Saccenti, E. (2022) The Power of Microbiome Studies: Some Considerations on Which Alpha and Beta Metrics to Use and How to Report Results. *Front Microbiol* **12**: 1–18.

King, G.M., Judd, C., Kuske, C.R., and Smith, C. (2012) Analysis of stomach and gut microbiomes of the Eastern oyster (*Crassostrea virginica*) from Coastal Louisiana, USA. *PLoS One* **7**:.

Klindworth, A., Pruesse, E., Schweer, T., Peplies, J., Quast, C., Horn, M., and Glöckner, F.O. (2013) Evaluation of general 16S ribosomal RNA gene PCR primers for classical and next-generation sequencing-based diversity studies. *Nucleic Acids Res* **41**: 1–11.

Kodama, Y. and Watanabe, K. (2004) *Sulfuricurvum kujiense* gen. nov., sp. nov., a facultatively anaerobic, chemolithoautotrophic, sulfur-oxidizing bacterium isolated from an underground crude-oil storage cavity. *Int J Syst Evol Microbiol* **54**: 2297–2300.

Kremer, N., Koch, E.J., El Filali, A., Zhou, L., Heath-Heckman, E.A.C., Ruby, E.G., and McFall-Ngai, M.J. (2018) Persistent interactions with bacterial symbionts direct mature-host cell morphology and gene expression in the squid-*Vibrio* symbiosis. *mSystems* **3**: 1–17.

Lathlean, J.A., Ayre, D.J., and Minchinton, T.E. (2014) Estimating latitudinal variability in extreme heat stress on rocky intertidal shores. *J Biogeogr* **41**: 1478–1491.

Lau, N.S., Ting, S.Y., Sam, K.K., Janaranjani, M., Wong, S.C., Wu, X., et al. (2022) Comparative analyses of *Scylla olivacea* gut microbiota composition and function suggest the capacity for polyunsaturated fatty acid biosynthesis. *Microb Ecol* 1–14.

Lee, Y.Y., Galano, J.M., Leung, H.H., Balas, L., Oger, C., Durand, T., and Lee, J.C.Y. (2020) Nonenzymatic oxygenated metabolite of docosahexaenoic acid, 4(RS)-4-$F_{4t}$-neuroprostane, acts as a bioactive lipid molecule in neuronal cells. *FEBS Lett* **594**: 1797–1808.

Lee, Y.Y. and Lee, J.C.-Y. (2018) LC-MS/MS Analysis of Lipid Oxidation Products in Blood and Tissue Samples. In *Clinical Metabolomics: Methods and Protocols*. Giera, M. (ed). Springer Science+Business Media, LLC.

Lent, C.M. (1969) Adaptations of the ribbed mussel, Modiolus demissus (Dillvvyn), to the intertidal habitat. *Integr Comp Biol* **9**: 283–292.

Lenth, R. V. (2023) emmeans: Estimated Marginal Means, aka Least-Squares Means.

Leung, K.S., Galano, J.M., Durand, T., and Lee, J.C.Y. (2015) Current development in non-enzymatic lipid peroxidation products, isoprostanoids and isofuranoids, in novel biological samples. *Free Radic Res* **49**: 816–826.

Li, J., Bates, K.A., Hoang, K.L., Hector, T.E., Knowles, S.C.L., and King, K.C. (2022) Experimental temperatures shape host microbiome diversity and composition. *Glob Chang Biol* **00**: 1–16.

Li, Y.F., Yang, N., Liang, X., Yoshida, A., Osatomi, K., Power, D., et al. (2018) Elevated seawater temperatures decrease microbial diversity in the gut of *Mytilus coruscus*. *Front Physiol* **9**: 839.

Lin, H. and Peddada, S. Das (2020) Analysis of compositions of microbiomes with bias correction. *Nat Commun* **11**: 1–11.

Liu, M., Li, Q., Tan, L., Wang, L., Wu, F., Li, L., and Zhang, G. (2023) Host-microbiota interactions play a crucial role in oyster adaptation to rising seawater temperature in summer. *Environ Res* **216**:.

Lokmer, A. and Wegner, K.M. (2015) Hemolymph microbiome of Pacific oysters in response to temperature, temperature stress and infection. *ISME J* **9**: 670–682.

de Lorgeril, J., Lucasson, A., Petton, B., Toulza, E., Montagnani, C., Clerissi, C., et al. (2018) Immune-suppression by OsHV-1 viral infection causes fatal bacteraemia in Pacific oysters. *Nat Commun* **9**:.

Ma, K., Chen, S., Wu, Y., Ma, Y., Qiao, H., Fan, J., and Wu, H. (2022) Dietary supplementation with microalgae enhances the zebrafish growth performance by modulating immune status and gut microbiota. *Appl Microbiol Biotechnol* **106**: 773–788.

Maher, R.L., Schmeltzer, E.R., Meiling, S., McMinds, R., Ezzat, L., Shantz, A.A., et al. (2020) Coral microbiomes demonstrate flexibility and resilience through a reduction in community diversity following a thermal stress event. *Front Ecol Evol* **8**: 555698.
Mallick, H., Franzosa, E.A., Mclver, L.J., Banerjee, S., Sirota-Madi, A., Kostic, A.D., et al. (2019) Predictive metabolomic profiling of microbial communities using amplicon or metagenomic sequences. *Nat Commun* **10**: 1–11.
Mallott, E.K., Skovmand, L.H., Garber, P.A., and Amato, K.R. (2022) The fecal metabolome of black howler monkeys (*Alouatta pigra*) varies in response to seasonal dietary changes.
Marangon, E., Laffy, P.W., Bourne, D.G., and Webster, N.S. (2021) Microbiome-mediated mechanisms contributing to the environmental tolerance of reef invertebrate species. *Mar Biol* **168**: 1–18.
Marshall, D.J., Dong, Y., McQuaid, C.D., and Williams, G.A. (2011) Thermal adaptation in the intertidal snail *Echinolittorina malaccana* contradicts current theory by revealing the crucial roles of resting metabolism. *J Exp Biol* **214**: 3649–3657.
Marshall, D.J. and McQuaid, C.D. (2011) Warming reduces metabolic rate in marine snails: Adaptation to fluctuating high temperatures challenges the metabolic theory of ecology. *Proc R Soc B Biol Sci* **278**: 281–288.
Masasa, M., Kushmaro, A., Nguyen, D., Chernova, H., Shashar, N., and Guttman, L. (2023) Spatial Succession Underlies Microbial Contribution to Food Digestion in the Gut of an Algivorous Sea. *Am Soc Microbiol*.
Maurice, C.F., Cl Knowles, S., Ladau, J., Pollard, K.S., Fenton, A., Pedersen, A.B., and Turnbaugh, P.J. (2015) Marked seasonal variation in the wild mouse gut microbiota. *ISME J* **9**: 2423–2434.
McDevitt-Irwin, J.M., Garren, M., McMinds, R., Vega Thurber, R., and Baum, J.K. (2019) Variable interaction outcomes of local disturbance and El Niño-induced heat stress on coral microbiome alpha and beta diversity. *Coral Reefs* **38**: 331–345.
McKnight, D.T., Huerlimann, R., Bower, D.S., Schwarzkopf, L., Alford, R.A., and Zenger, K.R. (2019) Methods for normalizing microbiome data: An ecological perspective. *Methods Ecol Evol* **10**: 389–400.
Mcmahon, B.R. (1988) Physiological responses to oxygen depletion in intertidal animals. *Integr Comp Biol* **28**: 39–53.
McMurdie, P.J. and Holmes, S. (2013) Phyloseq: An R Package for reproducible interactive analysis and graphics of microbiome census data. *PLoS One* **8**:.
Mekuchi, M., Asakura, T., Sakata, K., Yamaguchi, T., Teruya, K., and Kikuchi, J. (2018) Intestinal microbiota composition is altered according to nutritional biorhythms in the leopard coral grouper (Plectropomus leopardus). *PLoS One* **13**: 1–16.
Miller, E., Morel, A., Saso, L., and Saluk, J. (2014) Isoprostanes and neuroprostanes as biomarkers of oxidative stress in neurodegenerative diseases. *Oxid Med Cell Longev* **2014**:.
Monroig, Shu-Chien, A.C., Kabeya, N., Tocher, D.R., and Castro, L.F.C. (2022) Desaturases and elongases involved in long-chain polyunsaturated fatty acid biosynthesis in aquatic animals: From genes to functions. *Prog Lipid Res* **86**: 101157.
Le Moullac, G., Cheize, M., Gastineau, O., Daniel, J.Y., Le Coz, J.R., Huvet, A., et al. (2008) Ecophysiological and metabolic adaptations to sulphide exposure of the oyster *Crassostrea gigas*. *J Shellfish Res* **27**: 355–363.
Muñoz, K., Flores-Herrera, P., Gonçalves, A.T., Rojas, C., Yáñez, C., Mercado, L., et al. (2019) The immune response of the scallop *Argopecten purpuratus* is associated with changes in the host microbiota structure and diversity. *Fish Shellfish Immunol* **91**: 241–250.
Nakagawa, S., Saito, H., Tame, A., Hirai, M., Yamaguchi, H., Sunata, T., et al. (2017)

Microbiota in the coelomic fluid of two common coastal starfish species and characterization of an abundant *Helicobacter*-related taxon. *Sci Rep* **7**: 1–10.
Nearing, J.T., Douglas, G.M., Hayes, M., Macdonald, J., Desai, D., Allward, N., et al. (2022) Microbiome differential abundance methods produce disturbingly different results across 38 datasets. *Nat Commun* **13**: 342.
Neu, A.T., Hughes, I. V., Allen, E.E., and Roy, K. (2021) Decade-scale stability and change in a marine bivalve microbiome. *Mol Ecol* **30**: 1237–1250.
Ng, T.P.T., Lau, S.L.Y., Davies, M.S., Stafford, R., Seuront, L., Hutchinson, N., et al. (2021) Behavioral repertoire of high-shore littorinid snails reveals novel adaptations to an extreme environment. *Ecol Evol* **11**: 7114–7124.
Ng, T.P.T., Lau, S.L.Y., Seuront, L., Davies, M.S., Stafford, R., Marshall, D.J., and Williams, G.A. (2017) Linking behaviour and climate change in intertidal ectotherms: insights from littorinid snails. *J Exp Mar Bio Ecol* **492**: 121–131.
Nguyen, Q.P., Karagas, M.R., Madan, J.C., Dade, E., Palys, T.J., Morrison, H.G., et al. (2021) Associations between the gut microbiome and metabolome in early life. *BMC Microbiol* **21**: 1–19.
Nicastro, K.R., Zardi, G.I., McQuaid, C.D., Stephens, L., Radloff, S., and Blatch, G.L. (2010) The role of gaping behaviour in habitat partitioning between coexisting intertidal mussels. *BMC Ecol* **10**:.
Oksanen, J., Simpson, G.L., Blanchet, F.G., Kindt, R., Legendre, P., Minchin, P.R., et al. (2022) Vegan: community ecology package. *R Packag version 26-2*.
Pal, V.K., Bandyopadhyay, P., and Singh, A. (2018) Hydrogen sulfide in physiology and pathogenesis of bacteria and viruses. *IUBMB Life* **70**: 393–410.
Parris, D.J., Morgan, M.M., and Stewart, F.J. (2019) Feeding rapidly alters microbiome composition and gene transcription in the clownfish gut. *Appl Environ Microbiol* **85**: 1–15.
Petersen, C. and Round, J.L. (2014) Defining dysbiosis and its influence on host immunity and disease. *Cell Microbiol* **16**: 1024–1033.
Pierce, M.L. and Evan, J. (2019) Gut microbiomes of the eastern oyster (*Crassostrea virginica*) and the blue mussel (*Mytilus edulis*): Temporal variation and the influence of marine aggregate-associated microbial communities. *mSphere* **4**: e00730-19.
Pierce, M.L. and Ward, J.E. (2018) Microbial Ecology of the Bivalvia, with an Emphasis on the Family Ostreidae. *J Shellfish Res* **37**: 793–806.
Pimentel, Z.T., Dufault-Thompson, K., Russo, K.T., Scro, A.K., Smolowitz, R.M., Gomez-Chiarri, M., and Zhang, Y. (2021) Microbiome analysis reveals diversity and function of *Mollicutes* associated with the Eastern oyster, Crassostrea virginica. *mSphere* **6**: e00227-21.
Pita, L., Rix, L., Slaby, B.M., Franke, A., and Hentschel, U. (2018) The sponge holobiont in a changing ocean: from microbes to ecosystems. *Microbiome* **6**: 46.
Qi, Z. and Voit, E.O. (2017) Strategies for Comparing Metabolic Profiles: Implications for the Inference of Biochemical Mechanisms from Metabolomics Data. *IEEE/ACM Trans Comput Biol Bioinform* **14**: 1434–1445.
Quast, C., Pruesse, E., Yilmaz, P., Gerken, J., Schweer, T., Yarza, P., et al. (2013) The SILVA ribosomal RNA gene database project: Improved data processing and web-based tools. *Nucleic Acids Res* **41**: D590–D596.
Rädecker, N., Pogoreutz, C., Gegner, H.M., Cárdenas, A., Perna, G., Geißler, L., et al. (2022) Heat stress reduces the contribution of diazotrophs to coral holobiont nitrogen cycling. *ISME J* **16**: 1110–1118.
Raffaelli, D. and Hawkins, S. (1999) Intertidal ecology, 2nd ed. Kluwer Academic Publishers.
Rocca, J.D., Simonin, M., Blaszczak, J.R., Ernakovich, J.G., Gibbons, S.M., Midani, F.S., and

Washburne, A.D. (2019) The Microbiome Stress Project: Toward a global meta-analysis of environmental stressors and their effects on microbial communities. *Front Microbiol* **9**: 3272.
Roy, J., Galano, J.M., Durand, T., Le Guennec, J.Y., and Lee, J.C.Y. (2017) Physiological role of reactive oxygen species as promoters of natural defenses. *FASEB J* **31**: 3729–3745.
Samakraman, S., Williams, G.A., and Ganmanee, M. (2010) Spatial and temporal variability of intertidal rocky shore molluscs in Sichang Island, East Coast of Thailand. *Publ Seto Mar Biol Lab* **10**: 35–46.
Santoro, E.P., Borges, R.M., Espinoza, J.L., Freire, M., Messias, C.S.M.A., Villela, H.D.M., et al. (2021) Coral microbiome manipulation elicits metabolic and genetic restructuring to mitigate heat stress and evade mortality. *Sci Adv* **7**: 19–21.
Sargent, J.R. (1976) The Structure, Metabolism and Function of Lipids in Marine organisms. In *Biochemical and biophysical perspectives in marine biology*. Malins, D.C. and Sargent, J.R. (eds). New York: Academic Press, pp. 149–212.
Scanes, E., Parker, L.M., Seymour, J.R., Siboni, N., Dove, M.C., O'Connor, W.A., and Ross, P.M. (2021) Microbiomes of an oyster are shaped by metabolism and environment. *Sci Rep* **11**: 1–7.
Segata, N., Izard, J., Waldron, L., Gevers, D., Miropolsky, L., Garrett, W.S., and Huttenhower, C. (2011) Metagenomic biomarker discovery and explanation. *Genome Biol* **12**: R60.
Sepulveda, J. and Moeller, A.H. (2020) The effects of temperature on animal gut microbiomes. *Front Microbiol* **11**: 384.
Sharp, C. and Foster, K.R. (2022) Host control and the evolution of cooperation in host microbiomes. *Nat Commun* **13**: 1–15.
Sharp, K.H., Pratte, Z.A., Kerwin, A.H., Rotjan, R.D., and Stewart, F.J. (2017) Season, but not symbiont state, drives microbiome structure in the temperate coral *Astrangia poculata*. *Microbiome* **5**: 120.
Shaver, E.C., Shantz, A.A., McMinds, R., Burkepile, D.E., Thurber, R.L.V., and Silliman, B.R. (2017) Effects of predation and nutrient enrichment on the success and microbiome of a foundational coral. *Ecology* **98**: 830–839.
Shiu, J.H., Keshavmurthy, S., Chiang, P.W., Chen, H.J., Lou, S.P., Tseng, C.H., et al. (2017) Dynamics of coral-associated bacterial communities acclimated to temperature stress based on recent thermal history. *Sci Rep* **7**: 1–13.
Soen, Y. (2014) Environmental disruption of host-microbe co-adaptation as a potential driving force in evolution. *Front Genet* **5**: 168.
Sokolova, I.M. and Pörtner, H.O. (2001) Physiological adaptations to high intertidal life involve improved water conservation abilities and metabolic rate depression in *Littorina saxatilis*. *Mar Ecol Prog Ser* **224**: 171–186.
Sokolova, I.M., Sukhotin, A.A., and Lannig, G. (2011) Marine Animal Stress Response and Biomonitoring and Energy Budgets In Mollusks. In *Oxidative stress in aquatic ecosystems*. pp. 261–280.
Somero, G.N. (2002) Thermal physiology and vertical zonation of intertidal animals: Optima, limits, and costs of living. *Integr Comp Biol* **42**: 780–789.
Sorek, M., Díaz-Almeyda, E.M., Medina, M., and Levy, O. (2014) Circadian clocks in symbiotic corals: The duet between *Symbiodinium* algae and their coral host. *Mar Genomics* **14**: 47–57.
Stevick, R.J., Post, A.F., and Gómez-Chiarri, M. (2021) Functional plasticity in oyster gut microbiomes along a eutrophication gradient in an urbanized estuary. *Anim Microbiome* **3**:.

1147 Stillman, J.H. (2002) Causes and consequences of thermal tolerance limits in rocky intertidal
1148 porcelain crabs, genus *Petrolisthes*. *Integr Comp Biol* **42**: 790–796.
1149 Storey, K.B. and Storey, J.M. (2004) Oxygen Limitation and Metabolic Rate Depression. In
1150 *Functional Metabolism: Regulation and Adaptation*. John Wiley & Sons, Inc.
1151 Sussarellu, R., Fabioux, C., Camacho Sanchez, M., Le Goïc, N., Lambert, C., Soudant, P.,
1152 and Moraga, D. (2012) Molecular and cellular response to short-term oxygen variations
1153 in the Pacific oyster *Crassostrea gigas*. *J Exp Mar Bio Ecol* **412**: 87–95.
1154 Tremaroli, V. and Bäckhed, F. (2012) Functional interactions between the gut microbiota and
1155 host metabolism. *Nature* **489**: 242–249.
1156 Vandamme, P. and De Ley, J. (1991) Proposal for a new family, *Campylobacteraceae*. *Int J*
1157 *Syst Bacteriol* **41**: 451–455.
1158 Voolstra, C.R. and Ziegler, M. (2020) Adapting with microbial help: Microbiome flexibility
1159 facilitates rapid responses to environmental change. *BioEssays* **42**: 1–9.
1160 Walke, J.B., Becker, M.H., Krinos, A., Chang, E.A.B., Santiago, C., Umile, T.P., et al. (2021)
1161 Seasonal changes and the unexpected impact of environmental disturbance on skin
1162 bacteria of individual amphibians in a natural habitat. *FEMS Microbiol Ecol* **97**: 1–14.
1163 Wang, J., Ma, L.X., and Dong, Y.W. (2022) Coping with harsh heat environments: molecular
1164 adaptation of metabolic depression in the intertidal snail *Echinolittorina radiata*. *Cell*
1165 *Stress Chaperones*.
1166 Weiss, S., Xu, Z.Z., Peddada, S., Amir, A., Bittinger, K., Gonzalez, A., et al. (2017)
1167 Normalization and microbial differential abundance strategies depend upon data
1168 characteristics. *Microbiome* **5**: 1–18.
1169 Welker, A.F., Moreira, D.C., Campos, É.G., and Hermes-Lima, M. (2013) Role of redox
1170 metabolism for adaptation of aquatic animals to drastic changes in oxygen availability.
1171 *Comp Biochem Physiol - A Mol Integr Physiol* **165**: 384–404.
1172 Wickham, H. (2008) ggplot2: Elegant Graphics for Data Analysis, New York, USA: Springer
1173 Science+Business Media, LCC.
1174 Williams, G.A. and Morritt, D. (1995) Habitat partitioning and thermal tolerance in a tropical
1175 limpet, Cellana grata. *Mar Ecol Prog Ser* **124**: 89–103.
1176 Willis, A.D. (2019) Rarefaction, alpha diversity, and statistics. *Front Microbiol* **10**:.
1177 Yin, X., Chen, P., Chen, H., Jin, W., and Yan, X. (2017) Physiological performance of the
1178 intertidal Manila clam (*Ruditapes philippinarum*) to long-term daily rhythms of air
1179 exposure. *Sci Rep* **7**: 41648.
1180 Yonny, M.E., Rodríguez Torresi, A., Cuyamendous, C., Réversat, G., Oger, C., Galano, J.M.,
1181 et al. (2016) Thermal stress in melon plants: Phytoprostanes and phytofurans as
1182 oxidative stress biomarkers and the effect of antioxidant supplementation. *J Agric Food*
1183 *Chem* **64**: 8296–8304.
1184 Zaneveld, J.R., McMinds, R., and Thurber, R.V. (2017) Stress and stability: Applying the
1185 Anna Karenina principle to animal microbiomes. *Nat Microbiol* **2**:.
1186 Ziegler, M., Seneca, F.O., Yum, L.K., Palumbi, S.R., and Voolstra, C.R. (2017) Bacterial
1187 community dynamics are linked to patterns of coral heat tolerance. *Nat Commun* **8**: 1–8.
1188
1189

# Supplementary information

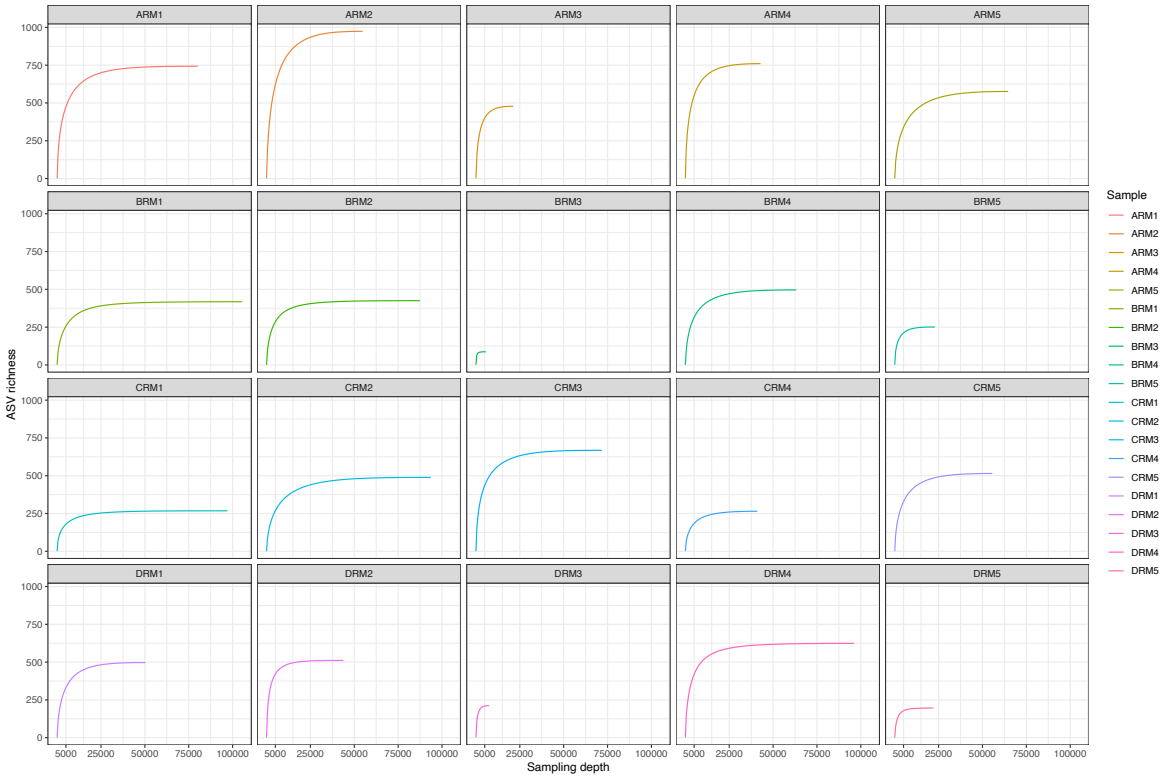


**Fig. S1. Rarefaction curves illustrating the ASVs captured against the sampling depth which was generated for each sample using their corresponding quality-filtered V3-V4 16SrRNA sequences**.

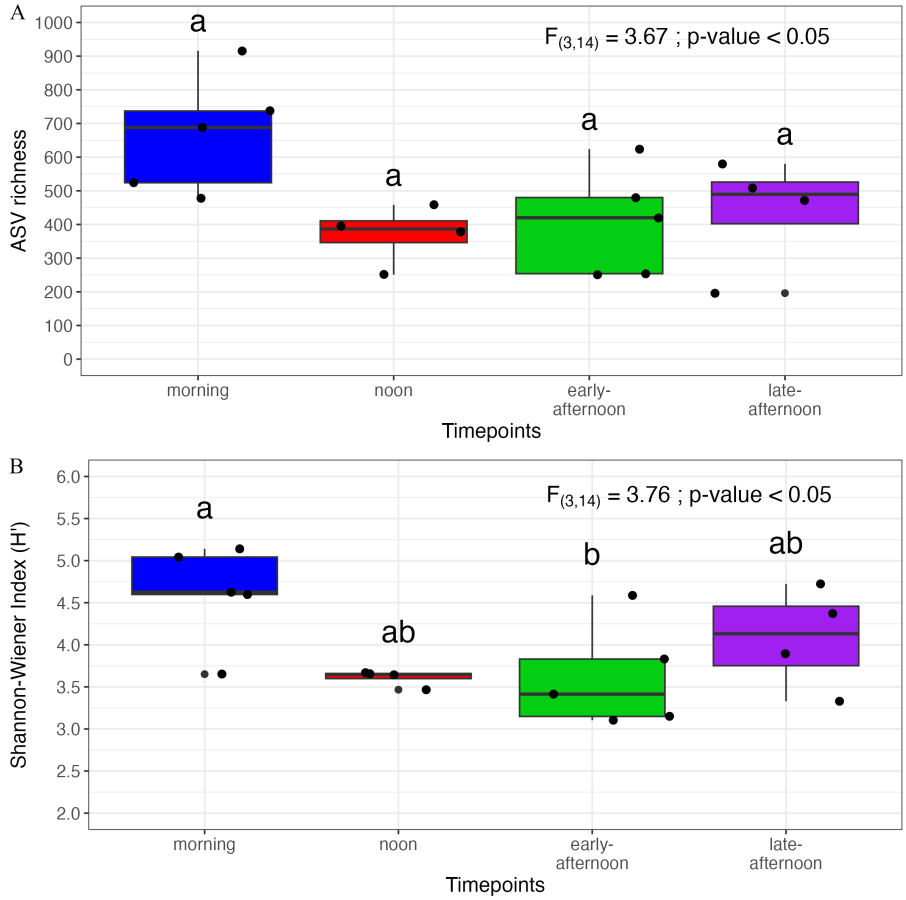


**Fig. S2. *I. nucleus*-associated microbiome ASV richness and Shannon-Wiener diversity across the emersion period.** Boxplot showing the alpha diversity index of (A) ASV richness, and (B) Shannon-Wiener index (H') of the oyster-associated microbiome at different timepoints. (Centre line represents the median; box limits indicate the first and third quartiles; the lower and upper whiskers indicate the smallest and largest values that within 1.5 times of the IQR (Inter-quartile range) from the first and third quartiles, respectively. The data points shown in each timepoint is replicate values. Statistical significance ($p < 0.05$) is indicated if the letters above each boxplot are different between any two timepoints.

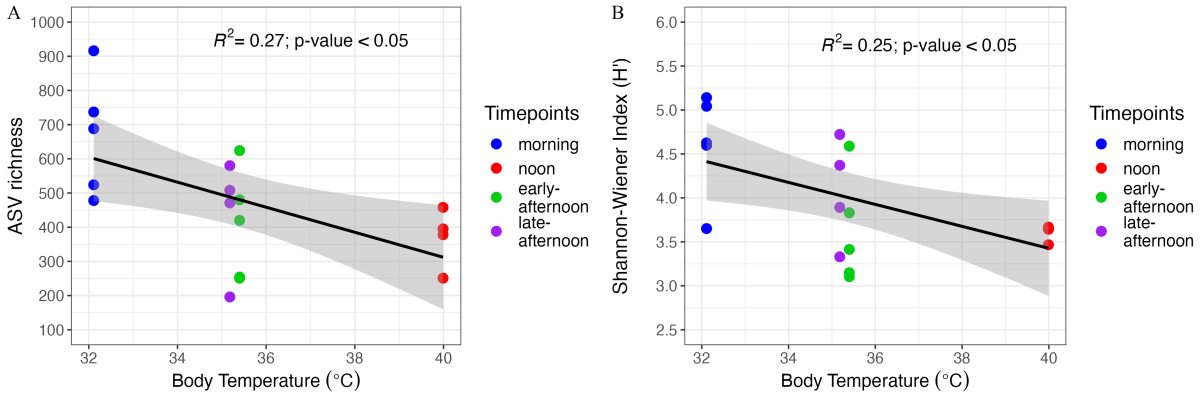


**Fig. S3. Variation in the alpha diversity indices of the *I. nucleus*-associated microbiome can be explained by the host body temperature.** Linear regression graph showing the relationship between average body temperature (from 10 random independent replicates collected at each timepoint) and (A) ASV richness (B) Shannon-Wiener index (H'). The

datapoints shown in each panel were the samples' replicates (n= 4-5) from their corresponding timepoint. The shaded grey area indicates a 95% confidence interval for the predicted regression line. Statistical result (least square regression analysis) is shown in the upper right within each panel.

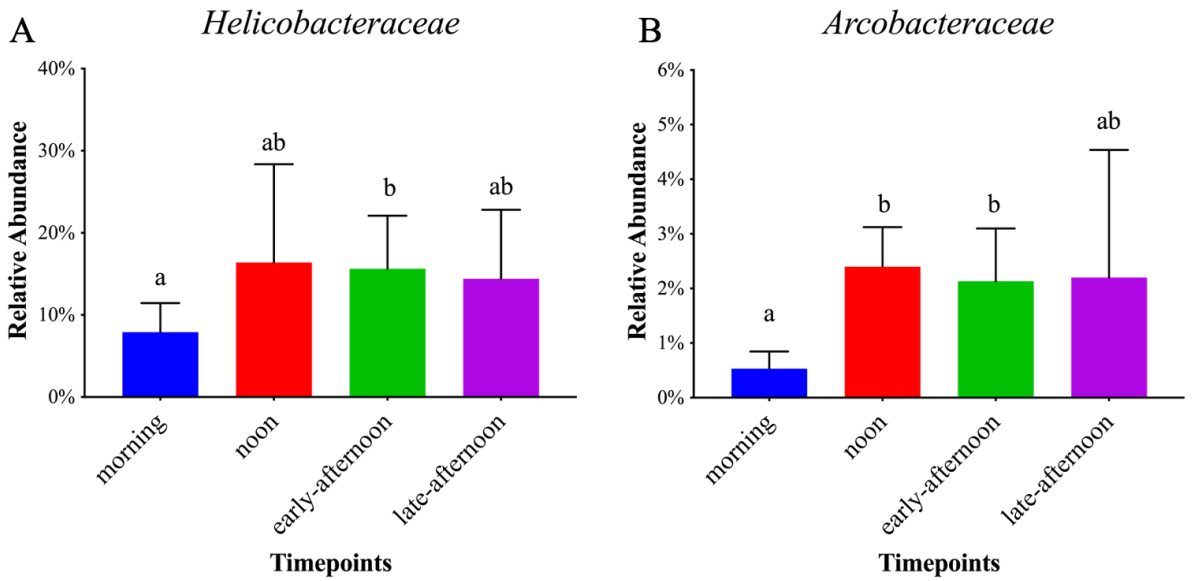


**Fig. S4. *Helicobacteraceae* and *Arcobacteraceae* mean relative abundance vary across the emersion period.** Bar graphs showing the two dominant family level taxa in *I. nucleus*'s gut microbiome at each timepoint: (A) *Helicobacteraceae* (B) *Arcobacteraceae*. Data are presented as mean relative abundance and + 1 standard deviation (error bar) for each taxon at the given timepoints. Statistical significance (p-value < 0.05) is indicated if the letters above each bar are different

.

1228 Table S1. Metadata describing the *Isognomon nucleus* samples' collected information

| Date | Time | Timepoints label | Replicates | Sample name | Body (mm) |
|---|---|---|---|---|---|
| 22.05.2019 | 0915 | morning | 1 | ARM1 | 12.9 |
| | | | 2 | ARM2 | 13.5 |
| | | | 3 | ARM3 | 15.2 |
| | | | 4 | ARM4 | 12.5 |
| | | | 5 | ARM5 | 13.7 |
| | 1230 | noon | 1 | BRM1 | 11.7 |
| | | | 2 | BRM2 | 11.3 |
| | | | 4 | BRM4 | 11.9 |
| | | | 5 | BRM5 | 12.4 |
| | 1612 | early-afternoon | 1 | CRM1 | 11.7 |
| | | | 2 | CRM2 | 12.9 |
| | | | 3 | CRM3 | 13.0 |
| | | | 4 | CRM4 | 12.0 |
| | | | 5 | CRM5 | 11.7 |
| | 1740 | late-afternoon | 1 | DRM1 | 11.8 |
| | | | 2 | DRM2 | 10.9 |
| | | | 4 | DRM4 | 11.1 |
| | | | 5 | DRM5 | 11.9 |

1229

1230 Table S2. Description of oxidized poly-unsaturated fatty acids (PUFA) products

| PUFA | Oxidized PUFA products |
|---|---|
| Arachidonic acid (ARA) | 5-$F_{2t}$-IsoP |
| | 15-$F_{2t}$-IsoP |
| Adrenic acid (AdA) | 7-$F_{2t}$-Dihomo-IsoP |
| | 17-$F_{2t}$-Dihomo-IsoP |
| Docosahexaenoic acid (DHA) | 4-$F_{4t}$-NeuroP |
| | 10-$F_{4t}$-NeuroP |
| | 13-$F_{4t}$-NeuroP |
| | 20-$F_{4t}$-NeuroP |
| α-Linolenic acid (ALA) | 9-$D_{1t}$-PhytoP |
| | 9-$F_{1t}$-PhytoP |
| | 16-$F_{1t}$-PhytoP |
| | 16-$B_{1t}$-PhytoP |
| Eicosapentaenoic acid (EPA) | 5-$F_{3t}$-IsoP |
| | 15-$F_{3t}$-IsoP |
| | 8-$F_{3t}$-IsoP |

1231